EFFECTS OF MISSING DATA ON ZONAL KINETIC ENERGY CALCULATIONS

by

Norman W. Stoldt
B. S., Pennsylvania State University
1966

SUBMITTED IN PARTIAL FULFILLMENT OF THE
REQUIREMENTS FOR THE DEGREE OF
MASTER OF SCIENCE
at the
MASSACHUSETTS INSTITUTE OF TECHNOLOGY

January, 1971

Signature of Author.....
Department of Meteorology, 18 January 1971

Certified by.....
Thesis Supervisor

Accepted by.....
Chairman, Departmental Committee on
Graduate Students

EFFECTS OF MISSING DATA ON ZONAL KINETIC ENERGY CALCULATIONS

by

NORMAN W. STOLDT

Submitted the the Department of Meteorology on 18 January 1971
in partial fulfillment of the requirement for the
degree of Master of Science

ABSTRACT

The effects of missing data upon zonal kinetic energy calculations are investigated by constructing clusters of alternate stations in the vicinity of certain primary stations in order to increase the number of observations. Individual terms in both the symmetrical and traditional forms of the zonal kinetic energy equation are evaluated. The results are compared with previous calculations in which the effects of missing data were not explicitly considered. An adjustment of approximately three to five percent in the total number of missing reports failed to detect any systematic errors in the observed mean wind fields and the lack of observations at various levels had only a marginal influence on the quantitative results. Additional bias in the data is discussed and some recommendations for further research are presented

Thesis Supervisor: Edward N. Lorenz
Title: Professor of Meteorology

TABLE OF CONTENTS

LIST OF TABLES

LIST OF FIGURES

CHAPTER I. INTRODUCTION

A. Background

With the advent of modern electronic data processing techniques and the realization of a sufficiently dense network of upper-air stations, observational studies perform an ever increasing role in the development and refinement of theoretical models of atmospheric processes. The beginning of modern day observational studies dates back to Priestly (1949) who demonstrated the feasibility of global computations by calculating upper-level horizontal transports of water vapor and sensible heat over Larkhill, England. That same year, horizontal momentum transports extending around latitude circles for selected upper levels were computed by Widger (1949). Two years later Mintz (1951), using geostrophic-wind data, performed calculations for the entire depth of the northern hemisphere. Subsequent momentum studies by Starr (1951) and Starr and White (1951, 1952), using only observed winds, firmly established the importance of large-scale eddies in maintaining the kinetic energy of the zonal flow, a concept first proposed by Jeffreys (1926). (For a recent discussion of this negative eddy viscosity concept and its applications to systems other than the terrestrial atmosphere see Starr, 1968 and Starr and Gaut, 1970.)

Following these pioneering investigations, the Planetary Circulations Project at M. I. T. has performed various observational

studies of the kinetic energy of the zonally-averaged flow, gradually increasing the size of the data sample to obtain a more detailed analysis of the energy budget and to refine the computational procedures. For a compilation of the major publications up to 1965 under this project, see Starr and Saltzman (1966).

Over the last several years, various members of the project have directed their attention to a thorough evaluation of the mean zonal kinetic energy balance based on five years of daily upper-air data from approximately 800 stations, located over the northern hemisphere and extending down to 20°S latitude. This collection of data is known as the MIT General Circulation Data Library and covers the five year period beginning May 1, 1958.

It is convenient to point out at this time that the term "zonal kinetic energy" or "kinetic energy" will be used interchangeably with the expression "kinetic energy of the zonally-averaged flow". Since this thesis pertains solely to the latter form of energy, the simplification should not confuse the reader.

To determine the best method of analysis and to test different computational techniques in handling the previously mentioned five years of data, preliminary calculations of the mean angular momentum and zonal kinetic energy balance were performed by Starr, Peixoto and Gaut (1970). Their findings were then utilized by others to study the zonal kinetic energy balance in greater detail. Starr, Peixoto and Sims (1970)

evaluated both the horizontal and the vertical energy conversion processes, the latter being obtained indirectly through continuity principles. In a similar manner, Sims (1969) considered the symmetrical form of the zonal kinetic energy equation as formulated by Starr and Gaut (1969). In addition, Sims (1970) investigated the horizontal transports of zonal kinetic due to Reynolds stresses acting across a boundary surface for various latitude walls in the northern hemisphere. An evaluation of the vertical transports of zonal kinetic energy by Reynolds stresses acting across various pressure surfaces in the northern hemisphere was accomplished by Rosen (1970, 1971). Finally, Walker (1969, 1970) used a 206 station subset to test the full station network for a possible bias introduced by the presence of a disproportionate number of land, versus sea, observation sites.

B. Statement of problem

A problem inherent with all observed-wind studies is that of missing data in the upper levels. To reduce the influence from stations having an excessively small number of observations at such levels, a cut-off criterion was applied in the previous studies for each of the horizontal levels at which observations existed. Thus a station was omitted at a level if it failed to possess some arbitrary percentage of the total possible observations at that level. While this procedure diminished the use of unrepresentative data, the customary lack of observations at high

altitudes still remained. (See Walker, 1969 for a complete listing of the number of observations per level at each of the 799 stations during the five year period.)

Among the possible reasons for missing reports, the two most frequently discussed in the literature are strong winds and severe weather. When strong winds prevail over an observation site, the radiosonde balloon is usually a considerable distance away from the site by the time it reaches the upper levels. In such cases, the balloon is either beyond the range of the instruments, or the elevation angle is so small and erratic that it is difficult, if not impossible, to recover the wind speed in the upper levels. Since only reported winds were used in the five year data sample, the data would appear to be biased in favor of light winds. Priestly and Troup (1964) have found evidence at individual stations, over short time periods, that the omission of 10 percent of the strongest winds at a particular level results in a disproportionate loss of wind observations possessing northward components. The occurence of severe weather in the form of heavy icing, thunderstorms etc., can prevent the successful launching of radiosonde equipment. Since these conditions are frequently associated with the weather patterns ahead of upper-level troughs, they would also appear to reduce the likelihood of obtaining wind measurements possessing northward components.

If such selectivity exists in the occurrence of missing data, then regardless of the cause, even a small number of missing reports

could introduce systematic errors in momentum and energy calculations. It is the purpose of this thesis to investigate the possibility of such errors in the zonal kinetic energy balance as evaluated from the five years of data.

CHAPTER II. OBSERVATIONAL MATERIAL

In order to increase the number of observations, clusters of alternate stations were constructed for certain primary stations. Assuming 400 km represents approximately one-tenth the wavelength of an average mid-latitude, upper-level wave, reports from alternate stations within this distance were taken to approximate the missing wind at the primary station. Walker's 206 station subset formed the basic station network. An attempt was then made to select suitable alternates at each site from the remaining stations in the original 799 station set. Because of the available station distribution, it was recognized at the outset that it would be impossible to find alternates for all of the stations. Nevertheless, clusters of alternate stations were found for 59 primary stations. The individual alternates in each cluster were ranked according to their proximity to the primary station. If two stations were located an equal distance away from the primary, the station with the greatest number of overall observations was given the higher ranking.

A complete station listing appears at the end of Chapter VI. The station distribution is shown in Fig. 1. Alternate stations are denoted by triangles, while all other stations are indicated by dots. The overwhelming majority of alternate station clusters are associated with land based stations. Practically no improvement could be made in the sparse data regions over the oceans. Moreover, alternate stations do not exist

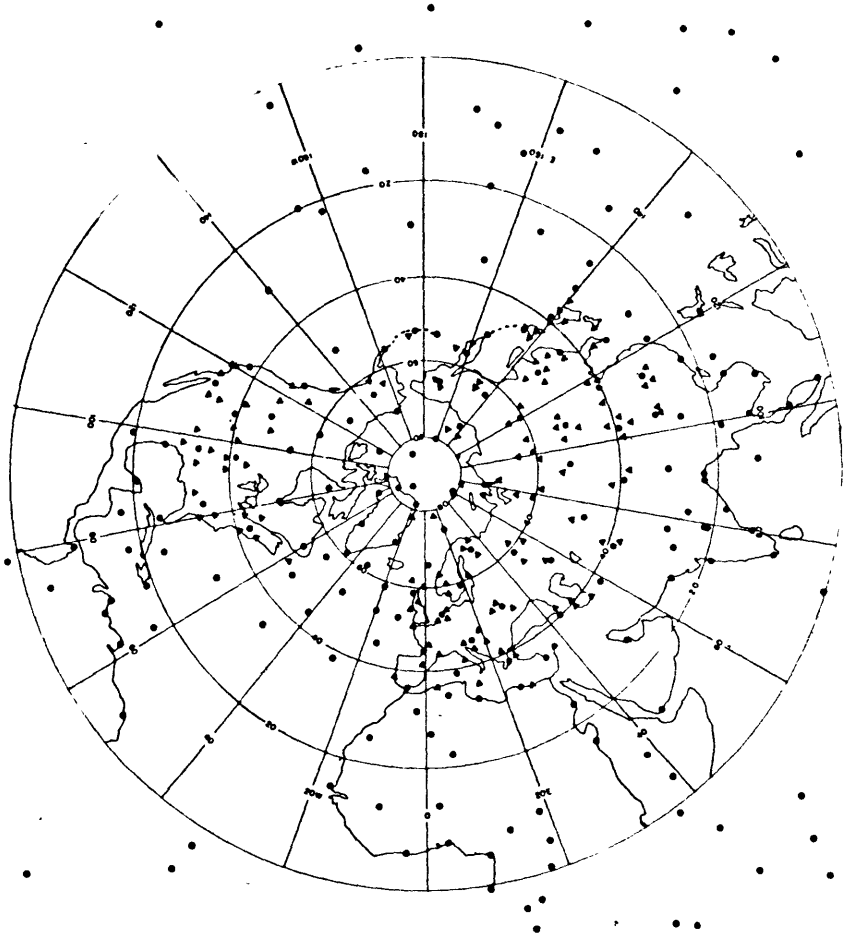

Fig. 1. Map of stations approximating the distribution used at all levels in the analysis. Alternate stations are shown by triangles; all other stations are represented by dots. Stations south of the equator were added to improve the analysis in the tropics. To augment the basic wind data, alternate station reports were substituted for missing reports at adjacent stations whenever possible.

Table 1. Summary of station distribution

Lat. (°N)	number of basic stations	number of alternate station clusters	total number of alternate stations
So of the equator	32	0	0
0-10	25	0	0
11-20	28	0	0
21-30	31	0	0
31-40	28	22	43
41-50	15	12	40
51-60	21	10	24
61-70	13	9	16
71-80	8	4	7
81-90	5	2	2
totals	206	59	164

south of 30°N, since Walker's set of stations included all available stations south of that latitude. Table 1 summarizes the distribution of the stations displayed in Fig. 1 in various latitude belts. The majority of the alternate station clusters lie between 30°N and 60°N, with the maximum number occurring between 31°N and 40°N. It is within these middle latitude zones that strong winds and severe weather should have the maximum effect in reducing the number of observations.

In substituting for the missing reports, so-called map tapes were used. These tapes list the original, daily reports for all 799 stations. The reports are arranged according to levels (1000, 950, 850, 700, 500, 400, 300, 200, 100, and 50 mb). When a primary station report was missing for a particular day and level, a wind was substituted from the first ranked alternate site for the corresponding day and level. If the wind was also missing at the first alternate, the remaining stations in the cluster were checked one by one in an attempt to substitute for the missing primary station report. This procedure was performed whenever an observation was missing at one of the 59 primary stations. Since a considerable amount of computer time is involved in searching through the data tapes to retrieve observations, it was decided to limit the study to a single season. The winter season, representing the five years of total number of observations for January, February and March was selected. A breakdown on the number of observations per level obtained for the 59

Table 2. Number of observations per level for the 59 primary stations. The numbers in parenthese represent the percent of missing observations compensated for by the added reports. The maximum number of observations possible at any one level is 26,609 (59 stations x 451 days).

level (mb)	number of original observations	number of observations added from alternate stations	total number of observations
50	6,551	3,919	10,470 (20)
100	14,755	5,357	20,112 (45)
200	18,167	4,247	22,414 (50)
300	20,261	3,327	23,588 (52)
400	20,309	3,439	23,748 (55)
500	23,317	2,142	25,459 (68)
700	24,411	1,542	25,953 (71)
850	24,375	1,680	26,055 (75)
900	6,587	1,868	8,445 (9)
950	6,529	1,604	8,133 (8)
1000	8,286	3,924	12,200 (21)

primary stations is given in Table 2. Since the maximum number of observations possible for the entire set of 206 stations at any one level is 92,906 (206 stations x 451 days), the total number of observations per level is increased by approximately three to five percent through the use of the alternate station reports.

CHAPTER III. QUANTITIES TO BE EVALUATED

Before introducing the various terms that are to be evaluated, it is first necessary to define some elementary operations. Any physical quantity can be considered as the sum of a mean value and a deviation from this mean. Applying this concept to the zonal wind component, u, we can write

$$u \equiv [u] + u^* . \tag{1}$$

The brackets represent an instantaneous spatial average along a latitude circle and are defined by

$$[\ ] = \frac{1}{2\pi}\int (\ )\, d\lambda \tag{2}$$

where λ denotes longitude. The quantity $(\ )^*$ signifies the instantaneous departure. Furthermore, u can be expressed as

$$u \equiv \overline{u} + u' \tag{3}$$

where the bar indicates averaging with respect to time and the prime represents the departure. Letting $u = \overline{u}$ in equation (1), we obtain

$$\overline{u} = [\overline{u}] + \overline{u}^* \tag{4}$$

where $[\overline{(\ )}]$ indicates a time space average, and $\overline{(\ )}^*$ represents the spatial deviation fromthis time average. In a similar manner, these operations can be applied to the meridional wind component, v. The latter is defined as positive toward the north, while u is positive toward the east. For additional comments on the physical interpretation of these operations, see Lorenz (1968).

According to Sims (1969) and the assumptions made therein, the time averaged symmetrical form of the zonal kinetic energy equation can be written as follows:

$$0 = \text{internal horizontal terms} \tag{5}$$

$$+\iint \frac{2\pi a^2}{g}\cos^2\phi(\Omega a\cos\phi)[\bar{v}]\frac{\partial}{a\partial\phi}\left\{\frac{[\bar{u}]}{a\cos\phi}\right\}a\,d\phi\,dP \qquad \{1\}$$

$$+\iint \frac{2\pi a^2}{g}\cos^2\phi[\bar{u}][\bar{v}]\frac{\partial}{a\partial\phi}\left\{\frac{[\bar{u}]}{a\cos\phi}\right\}a\,d\phi\,dP \qquad \{2\}$$

$$+\iint \frac{2\pi a^2}{g}\cos^2\phi[\bar{u}^*\bar{v}^*]\frac{\partial}{a\partial\phi}\left\{\frac{[\bar{u}]}{a\cos\phi}\right\}a\,d\phi\,dP \qquad \{3'\}$$

$$+\iint \frac{2\pi a^2}{g}\cos^2\phi[\overline{u'v'}]\frac{\partial}{a\partial\phi}\left\{\frac{[\bar{u}]}{a\cos\phi}\right\}a\,d\phi\,dP \qquad \{3''\}$$

plus the internal vertical terms

$$+\iint \frac{2\pi a^2}{g}\cos^2\phi(\Omega a\cos\phi)[\bar{\omega}]\frac{\partial}{\partial P}\left\{\frac{[\bar{u}]}{a\cos\phi}\right\}a\,d\phi\,dP \qquad \{4\}$$

$$+\iint \frac{2\pi a^2}{g}\cos^2\phi\,[\bar{u}]\,[\bar{\omega}]\,\frac{\partial}{\partial P}\left\{\frac{[\bar{u}]}{a\cos\phi}\right\}a\,d\phi\,dP \qquad \{5\}$$

$$+\iint \frac{2\pi a^2}{g}\cos^2\phi\left([\bar{u}^*\bar{\omega}^*]+[\overline{u'\omega'}]+[\bar{\tau}_F]\right)\frac{\partial}{\partial P}\left\{\frac{[\bar{u}]}{a\cos\phi}\right\}a\,d\phi\,dP \qquad \{6's\}$$

plus the vertical boundary terms at $\phi = \phi_1$

$$+\int \frac{2\pi a^2}{g} \cos^2\phi_1 (\Omega a \cos\phi_1) [\bar{v}] \frac{[\bar{u}]}{a\cos\phi_1} dP \qquad \{7\}$$

$$+\int \frac{2\pi a^2}{g} \cos^2\phi_1 [\bar{u}] [\bar{v}] \frac{[\bar{u}]}{a\cos\phi_1} dP \qquad \{8\}$$

$$+\int \frac{2\pi a^2}{g} \cos^2\phi_1 [\bar{u}^*\bar{v}^*] \frac{[\bar{u}]}{a\cos\phi_1} dP \qquad \{9'\}$$

$$+\int \frac{2\pi a^2}{g} \cos^2\phi_1 [\overline{u'v'}] \frac{[\bar{u}]}{a\cos\phi_1} dP \qquad \{9''\}$$

plus the horizontal boundary terms at $P = P_1$

$$-\int \frac{2\pi a^2}{g} \cos^2\phi (\Omega a \cos\phi) [\bar{\omega}] \frac{[\bar{u}]}{a\cos\phi} a d\phi \qquad \{10\}$$

$$-\int \frac{2\pi a^2}{g} \cos^2\phi [\bar{u}] [\bar{\omega}] \frac{[\bar{u}]}{a\cos\phi} a d\phi \qquad \{11\}$$

$$-\int \frac{2\pi a^2}{g} \cos^2\phi \left([\bar{u}^*\bar{\omega}^*] + [\overline{u'\omega'}] + [\bar{\tau}_F]\right) \frac{[\bar{u}]}{a\cos\phi} a d\phi \qquad \{12's\}$$

The horizontal coordinate, ϕ, denotes latitude and P, the vertical coordinate, is in units of pressure and satisfies the hydrostatic equation. Here 'a' represents the mean radius of the earth, while g is the acceleration due to gravity, and Ω is the rate of the earth's rotation. The quantity τ_F indicates the combined positive viscous effects of small-

scale turbulence and molecular motion, and $[\overline{\omega}]$ is the time and space averaged vertical velocity in pressure coordinates.

Since the various terms in (5) have been thoroughly discussed by Sims and others (Starr and Gaut, 1969), only the more significant features of the equation need be presented here. As written, (5) applies to a polar cap region in the northern hemisphere, bounded below by a smooth earth, above by the pressure surface p_1 and to the south by the equatorial plane. Each of the terms involves the product of some component of the mean angular momentum transport and the time and space averaged relative angular velocity, $[\overline{u}]/a\cos\phi$. The four components of the momentum transports are: that associated with the basic rotation Ω , that associated with the relative motion $[\overline{u}]$ and that associated with u' and $\overline{u}^*$. The latter represent the transient and standing eddy motions, respectively. For positive generation of mean zonal kinetic energy to occur, the transport of angular momentum must be up the angular velocity gradient. The boundary terms, $\{7\}$ through $\{9''\}$ and $\{10\}$ through $\{12's\}$ represent the transport of zonal kinetic energy accomplished by Reynolds stresses acting across free boundary surfaces. Nowhere in (5) is the direct advection of zonal kinetic energy represented. However, the process can be incorporated into the equation by performing various manipulations as shown by Starr and Sims (1970). Finally, it should be noted that the quantity $\left([\overline{u}^*\overline{\omega}^*] + [\overline{u'\omega'}] + [\overline{\tau}_F]\right)$ appearing in terms $\{6's\}$ and $\{12's\}$ represents a composite of different scales of vertical motion (including friction).

The methods used to evaluate this quantity, as well as $[\overline{\omega}]$, will be discussed in the next chapter.

Two additional quantities which appear solely in the traditional form of the equation (5) are also of interest. The first is the so-called fuv term,

$$\iint \frac{2\pi a^2}{g} \cos^2\phi \,(2\Omega \sin\phi)\,[\overline{v}]\,\frac{[\overline{u}]}{a\cos\phi}\, a\,d\phi\,dP \qquad \{1'\}$$

which represents the work done by the zonal component of the Coriolis force associated with $[\overline{v}]$. The other term is

$$\iint \frac{2\pi a^2}{g} \cos^2\phi \,(2\Omega \cos\phi)\,[\overline{\omega}]\,\frac{[\overline{u}]}{a\cos\phi}\, a\,d\phi\,dP \qquad \{4'\}$$

which represents the work done by the Coriolis force associated with $[\overline{\omega}]$. Of further interest are $2\pi a^2\cos^2\phi\,[\overline{u}^*\overline{v}^*]$ and $2\pi a^2\cos^2\phi\,[\overline{u'v'}]$. These last two sub-quantities signify the mean meridional transport of angular momentum by standing and transient eddies, respectively.

In the sections to follow, the various terms will generally be referred to only by the $\{\ \}$ expression to save space and time. For convenience, the numbering scheme employed in equation (5) and for the two Coriolis work terms is consistent with past energy studies (e. g., Starr, Peixoto and Sims, 1969 and Rosen, 1970).

CHAPTER IV. METHOD OF EVALUATION

A. Analysis scheme

The input tapes were prepared from the original map-tapes using substituted values for missing winds at the primary stations whenever possible. All reports on these modified tapes were screened to eliminate erroneous observations. Any u exceeding 99 m sec^{-1}, or v exceeding 79 m sec^{-1} were discarded. Time averages of u and v were next computed at the various pressure levels for each of the 59 stations. To preclude the influence of unrepresentative data, any particular station level possessing less than 30 percent of the total number of observations possible was discarded. However, it was necessary to reduce this value to 10 percent for some stations located in sparse data regions in order to retain a significant number of stations for analysis. The covariances of the temporal deviations, $u'v'$, were then calculated and averaged over time to yield $\overline{u'v'}$.

Merging the data from all 206 stations, grid point values were determined for $\overline{u}$, $\overline{v}$ and $\overline{u'v'}$ at every ten degrees of latitude and longitude, except near the pole where the spacing was reduced to five degree intervals. After obtaining the time averaged grid point values, the zonally averaged quantities, $[\overline{u}]$, $[\overline{v}]$, $[\overline{u'v'}]$ and $[\overline{u}^*\overline{v}^*]$ were computed at two degree intervals for each of the 20 pressure levels used in the calculations. Lower level values were used as an initial guess in cases

when observations were not available for the next higher level.

All computations, including the determination of grid point values, were entirely machine processed. The final analyzed quantities were printed out by the computer in the form of meridional cross sections. The cross sections were then redrafted by hand so they could be presented herein.

The programs for the actual computations were written by Travelers Research Center, Inc. (TRC), using ANAL 68. ANAL 68 is a high speed programming language developed by TRC to facilitate the handling of a variety of different analysis schemes on two-dimensional fields. The computations themselves were performed at the ESSA Geophysical Fluid Dynamics Laboratory at Princeton University on a UNIVAC 1108 computer. See Frazier et al. (1968) for further discussion on the basic techniques employed.

B. Computational techniques

The mean vertical motion $[\bar{\omega}]$ is determined indirectly from $[\bar{v}]$. Considering the net mass between latitude circles as being conserved, one can write a mass-flow stream function ψ as follows:

$$2\pi a \cos\phi [\bar{v}] = g \frac{\partial \psi}{\partial p} \tag{6}$$

$$2\pi a^2 \cos\phi [\bar{\omega}] = -g \frac{\partial \psi}{\partial \phi} \tag{7}$$

from which $[\bar{\omega}]$ can be obtained.

A method must also be devised to evaluate the quantity $\left([\bar{u}^*\bar{\omega}^*] + [\overline{u'\omega'}] + [\bar{\tau}_F]\right)$, which appears in terms $\{6's\}$ and $\{12's\}$. To accomplish this task a stream function χ is written for the absolute angular momentum, by considering non-divergent flow in a mean meridional plane. The result is

$$2\pi a^2 \cos^2\phi [\bar{\tau}_{\phi\lambda}] = \frac{\partial \chi}{\partial p} \tag{8}$$

$$2\pi a^3 \cos^2\phi [\bar{\tau}_{p\lambda}] = -g \frac{\partial \chi}{\partial \phi} \tag{9}$$

where $\tau_{\phi\lambda}$ and $\tau_{p\lambda}$ represent the total linear momentum transports per unit area, or the mean stresses, across latitude walls and pressure surfaces, respectively.

By neglecting the horizontal wind shears, the transport of total momentum per unit area across a latitude wall can be written as

$$[\bar{\tau}_{\phi\lambda}] = -\Omega a \cos\phi [\bar{v}] + [\bar{v}][\bar{u}] + [\bar{u}^*\bar{v}^*] + [\overline{u'v'}] \tag{10}$$

A somewhat similar expression for the vertical transport of total angular momentum can also be formulated. However, the wind shears in the vertical play a more significant role and can not be neglected. The result is

$$[\bar{\tau}_{p\lambda}] = -\Omega a \cos\phi [\bar{\omega}] + [\bar{u}][\bar{\omega}] + [\bar{u}^*\bar{\omega}^*] + [\overline{u'\omega'}] + [\bar{\tau}_F] \quad (11)$$

Equation (10) can be evaluated directly from the mean wind fields previously discussed. Hence upon integrating (8), the stream function χ is obtained, and consequently $[\bar{\tau}_{p\lambda}]$ is known. The combined value of the vertical eddies and $[\bar{\tau}_F]$ can now be solved for by using (11).

The observed vertical mass averaged of $[\bar{v}]$ was not zero as required by continuity requirements. It was therefore necessary to normalize the values of $[\bar{v}]$, so they would be more representative of actual atmospheric processes and not produce erroneous results in the calculations. This was achieved by simply subtracting the vertical mass average of $[\bar{v}]$ from the analyzed value of $[\bar{v}]$ at each pressure level. The procedure can be written as

$$[\bar{v}]_{NORMALIZED} = [\bar{v}]_{ANAL} - \frac{1}{p_o}\int_0^p [\bar{v}]\, dp \quad (12)$$

where p_o represents the surface pressure.

This then is a brief review of the procedures used to evaluate the various quantities of interest from the observations. Except for utilizing substituted reports to augment the basic wind data, the computations were performed in a manner identical to previous calculations (Sims, 1969 and Rosen, 1970) so that the effects of missing data could be studied.

CHAPTER V. PRESENTATION OF RESULTS

A. Basic quantities

In the figures and tables to follow, the values in column I were computed using alternate station reports in place of missing primary reports whenever possible. These values are to be compared with the results in column II, which were obtained without substituting for the missing data. All values apply to a 15 month winter season only.

The meridional disturibution of the mean zonal velocity, $[\overline{u}]$, is shown in the top two panels of Fig. 2. The two cross sections are virtually identical. While the use of substituted reports appears to have no effect on the values of $[\overline{u}]$, a couple of points should be noted. One, the maximum value of $[\overline{u}]$ occurs just south of 30°N, in a region where no alternate stations exist. Furthermore, during the winter season the strongest portions of the mean jet are found just east of the Asian and North American continents, two areas where the number of alternate stations are few (see Fig. 1). Still, judging from the number of reports added per level (Table 2), any signficant bias due to missing data should have been detected.

The mean meridional velocity, $[\overline{v}]$, is obtained from averaging relatively large values of v having opposite sign. Hence a greater uncertainty must be associated with estimates of $[\overline{v}]$ than those of $[\overline{u}]$. It has been shown that $[\overline{v}]$ is rather sensitive to observational sampling

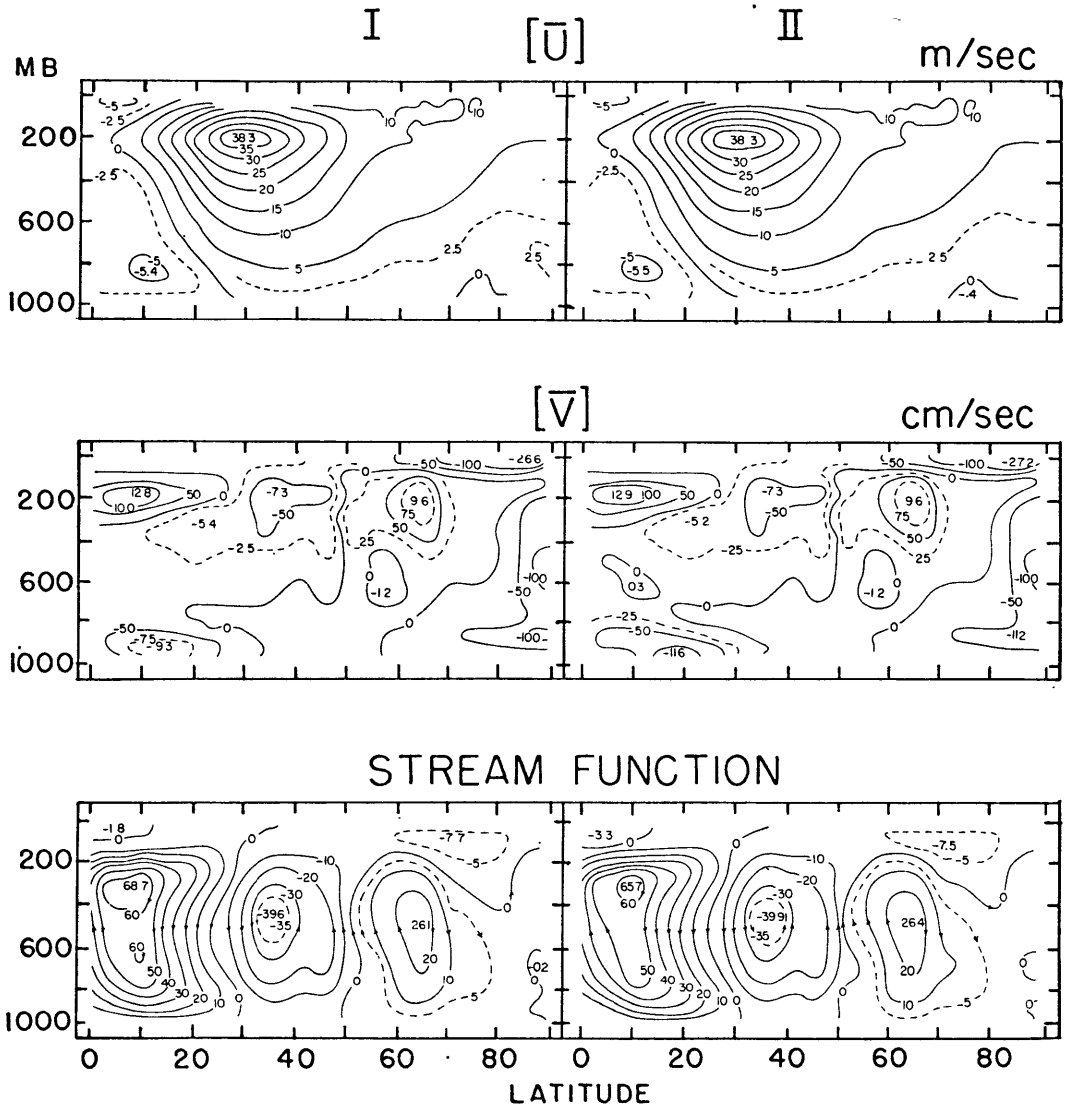

Fig. 2. Vertical meridional cross sections through the atmosphere displaying the mean velocity components and stream function. The latter quantity was obtained from $[\bar{v}]$ through mass continuity considerations and is in units of 10^{12} g sec^{-1}. The values in column I were computed using alternate station reports in place of missing primary station reports whenever possible. These values are to be compared with the results in column II, which were obtained using the original station reports.

(Starr, Peixoto and Gaut, 1970). It is somewhat surprising then, that the two meridional cross sections of $[\overline{v}]$ (second row of panels in Fig. 2) are so nearly identical. Only a very minor difference exists between the two panels in the lower levels. In the upper levels, no distinguishable change occurs by using additional reports. Due to smoothing, or some other feature in the objective analysis scheme, some differences show up south of 30°N, where no alternate stations exist.

Values of the vertical mass average of $[\overline{v}]$ computed at every two degrees of latitude are contained in Table 3 and plotted in the top two panels of Fig. 3. Viewing the computations of $[\overline{v}]$ in Table 3, the negative values between 20°N and 46°N have generally decreased in absolute value through the use of substituted reports. From mass continuity considerations, the values of $[\overline{v}]$ in both columns should be approximately zero. The large negative deviations in Fig. 3 and Table 3 indicate a fictitious southward transport of mass. A closer comparison between the panels depicting $[\overline{v}]$ in Fig. 2 and Fig. 3 reveals that the large negative deviations in Fig. 3 coin cide with latitide zones in Fig. 2 where the meridional velocity possesses a southward maximum. The magnitude of these deviations can be used as an indication of the reliability of the $[\overline{v}]$'s at the different latitudes. The maximum mid-latitude deviation appearing in column I and column II of Table 3 are 23 and 24 cm sec^{-1}, respectively. These values are comparable to those found in similar observational studies of the general circulation (e. g. Tucker, 1959; Palmen and Vuorela,

Table 3. Vertically averaged values of the mean meridional velocity and horizontal momentum transports.

Lat. (°N)	$[\bar{v}]$ cm sec^{-1}		$[\overline{v^*v^*}]\cos^2\phi$ 10^4cm^{2}sec^{-2}		$[\overline{u'v'}]\cos^2\phi$ 10^4cm^{2}sec^{-2}	
	I	II	I	II	I	II
0	-0.69	3.98	-1.28	-1.20	-0.44	-0.44
2	-0.12	4.36	-1.43	-1.29	0.09	-0.18
4	0.27	4.94	-1.48	-1.41	0.53	0.30
6	-1.91	4.55	-1.30	-1.39	1.17	0.87
8	-2.92	1.46	-1.17	-1.23	1.95	1.56
10	-4.95	-2.47	-0.83	-0.90	2.90	2.50
12	-9.90	-6.49	-0.43	-0.60	4.02	3.45
14	-13.2	-11.4	-0.09	-0.27	5.14	4.49
16	-15.3	-16.2	0.43	0.19	6.25	5.65
18	-16.6	-18.5	0.89	0.71	7.28	6.73
20	-19.7	-21.6	1.43	1.27	8.13	7.70
22	-20.7	-23.5	2.23	1.90	8.80	8.44
24	-18.3	-21.9	2.99	2.65	9.29	9.00
26	-17.4	-19.6	3.26	3.18	9.81	9.45
28	-18.4	-19.6	3.27	3.34	10.1	9.83
30	-21.1	-20.4	2.67	3.21	9.94	9.97
32	-24.0	-23.0	2.22	2.67	9.37	9.64
34	-23.5	-25.0	2.20	2.20	8.43	8.97
36	-22.2	-23.9	2.38	2.25	7.40	7.99
38	-17.5	-20.7	2.11	2.37	6.30	6.83
40	-12.4	-15.9	1.84	2.13	5.08	5.65
42	-12.9	-13.2	1.62	1.84	4.15	4.56
44	-18.0	-17.5	1.19	1.49	3.40	3.71
46	-16.1	-17.1	0.57	0.90	2.73	3.00
48	4.38	1.65	-0.30	0.17	2.19	2.39
50	22.5	21.5	-0.48	-0.25	1.70	1.90
52	19.9	22.2	-0.98	-0.66	1.20	1.44
54	10.5	13.8	-1.45	-1.26	0.75	0.90
56	8.53	9.31	-1.60	-1.55	0.31	0.50
58	11.6	10.6	-1.66	-1.64	-0.11	-0.09
60	15.4	13.3	-1.64	-1.64	-0.33	-0.22
62	20.6	17.2	-1.54	-1.58	-0.37	-0.35
64	24.3	22.7	-1.44	-1.51	-0.39	-0.40
66	17.9	22.0	-1.19	-1.32	-0.34	-0.39
68	2.65	9.57	-0.97	-1.07	-0.38	-0.37
70	-7.36	-3.56	-0.73	-0.84	-0.31	-0.34
72	-9.35	-9.51	-0.45	-0.58	-0.20	-0.25
74	-13.0	-14.0	-0.24	-0.30	-0.10	-0.13
76	-16.1	-16.2	-0.11	-0.15	0.02	-0.05
78	-20.6	-18.5	-0.03	-0.05	0.04	0.01
80	-26.8	-22.5	0	0	0.05	0.04
82	-39.6	-37.7	0	0	0.04	0.04
84	-63.8	-63.5	0	0	0.02	0.02
86	-79.5	-76.6	0	0	0	0.01
88	-77.8	-81.4	0	0	0	0

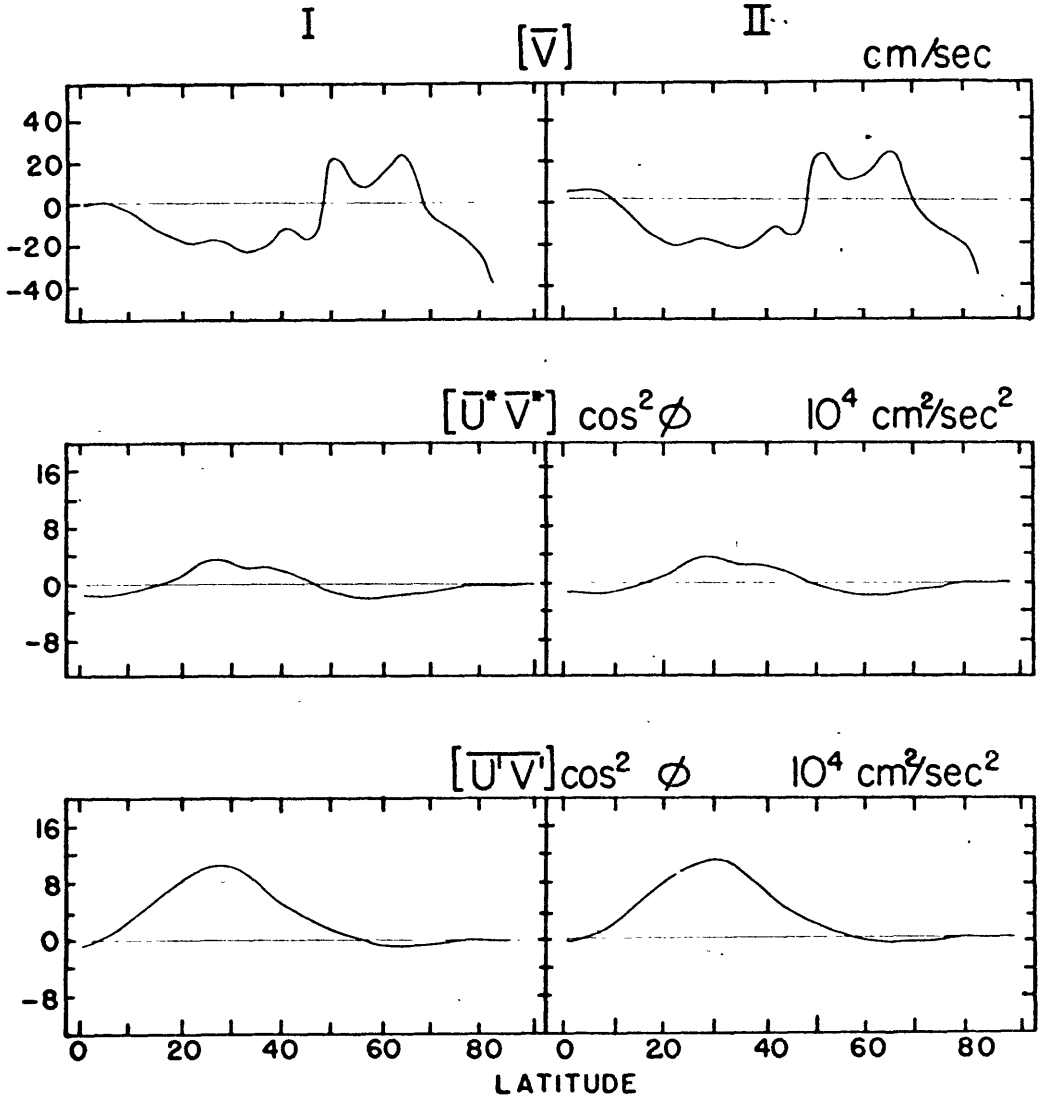

Fig. 3. Profiles of vertical integrals depicting the mean meridional velocity (top two panels) and the mean meridional transport of relative angular momentum by standing eddies (middle two panels) and transient eddies (bottom two panels). The momentum transports need to be multiplied by $2\pi a^2$ to be in the proper units. The values in column I were calculated from the augmented wind data, while the results shown in column II were obtained from the original data.

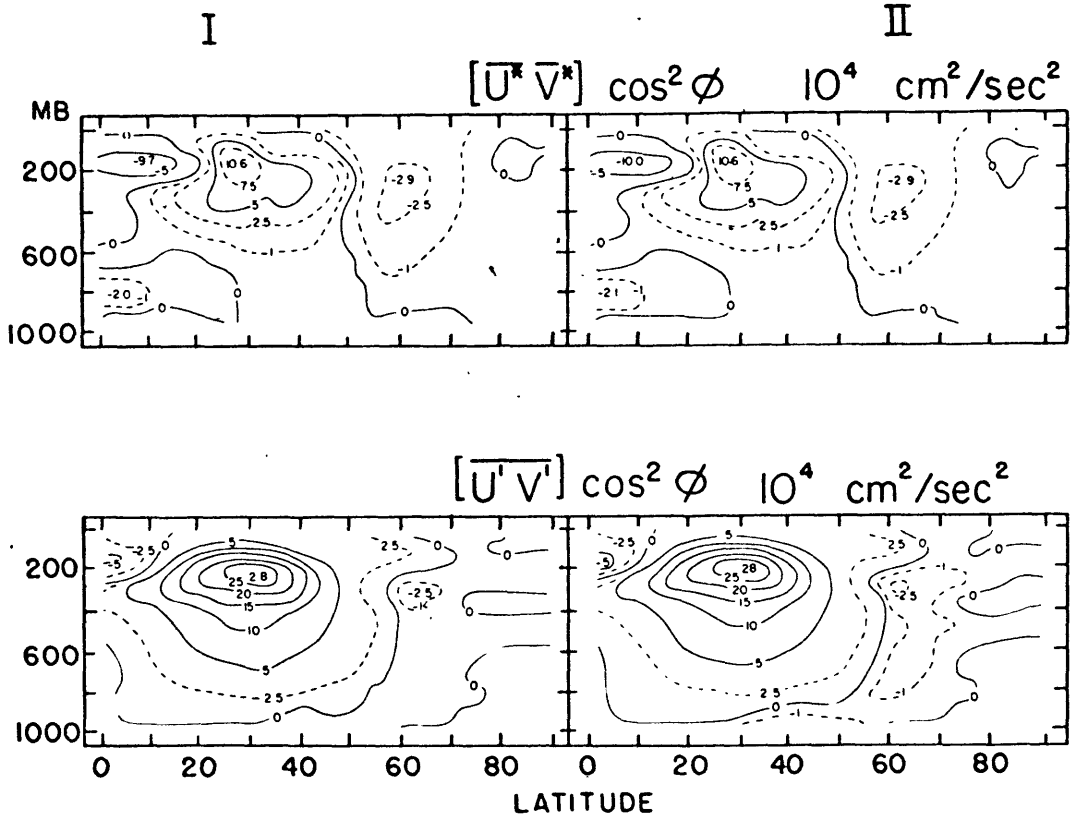

Fig. 4. Vertical meridional cross sections through the atmosphere showing the distribution of the mean meridional transport of angular momentum by standing eddies (top two panels) and transient eddies (bottom two panels). Both eddy transports need to be multiplied by $2\pi a^2$ to be in the proper units. Values in column I were computed using alternate station reports in place of missing primary station reports whenever possible. Values in column II were obtained using only the original station reports.

1963; and Vuorela and Tuominen, 1964).

The mass stream function is presented in the bottom two panels of Fig. 2. Minus values indicate counterclockwise circulation. The units are 10^{12} g sec^{-1}. Some small differences in the two panels can be detected. The indirect Ferrel cell has shifted its position slightly to the south. At the same time, the upper and lower portions of the tropical Hadley cell have increased in area and strength by using alternate station reports.

Fig. 4 shows cross sections through the atmosphere of the mean horizontal transport of relative angular momentum by the action of standing eddies (top two panels) and transient eddies (bottom two panels). The units are 10^{4} cm^{2} sec^{-2}. Positive values indicate northward momentum transport. Table 3 contains values of the vertical integral of the eddy quantities shown in Fig. 4. The meridional profiles of these integrals are displayed in the last two rows of panels in Fig. 3. The transports shown in the two figures and Table 3 need to be multiplied by $2\pi a^2$ to be in proper units. The values of the two eddy momentum transports demonstrate little change as a result of substituting for missing data. In fact, the values shown in Table 3 and Fig. 4 do not differ significantly from previous results based upon the full 799 station set (Macdonald and Frazier, 1969).

B. Internal horizontal processes

1. Evaluation of term $\{1'\}$:

$$\iint \frac{2\pi a^2}{g} \cos^2\phi \,(2\Omega \sin\phi)\,[\bar{v}]\,\frac{[\bar{u}]}{a\cos\phi}\, a\,d\phi\,dP$$

From the previous discussion of $[\bar{v}]$, one would expect that any variation in $\{1'\}$ due to missing data would be primarily the result of changes in $[\bar{v}]$. Small changes in $[\bar{v}]$ should have the greatest effect on $\{1'\}$ in regions of large $[\bar{u}]$'s. The presence of the trigonometric factor $\cos\phi\sin\phi$ also acts to enhance any mid-latitude changes in $[\bar{v}]$.

The meridional distribution of the integrand of $\{1'\}$ is shown in the top two rows of panels in Fig. 5a. Both the upper-level area of negative generation adjacent to the mean jet and the considerable weaker area of positive generation located below it occur in a region where the number of alternate station clusters is a maximum. Consequently, any effects from using substituted data should be more discernible in these two areas. The central value in the lower level area is slightly reduced by using the substituted reports, but the magnitude of this change is insufficient to indicate any bias from missing data due to severe weather, or to any other cause. The values in the upper-level area, where presumably strong winds would also tend to reduce the number of observations, show even less effect through the use of alternate station reports.

The computed value of $\{1'\}$ for atmospheric volumes of various depth is given in Table 4. The horizontal limits of integration are fixed at the pole and the equator. For the vertical integral, the lower limit is fixed at the 1013 mb pressure surface, while the upper limit is

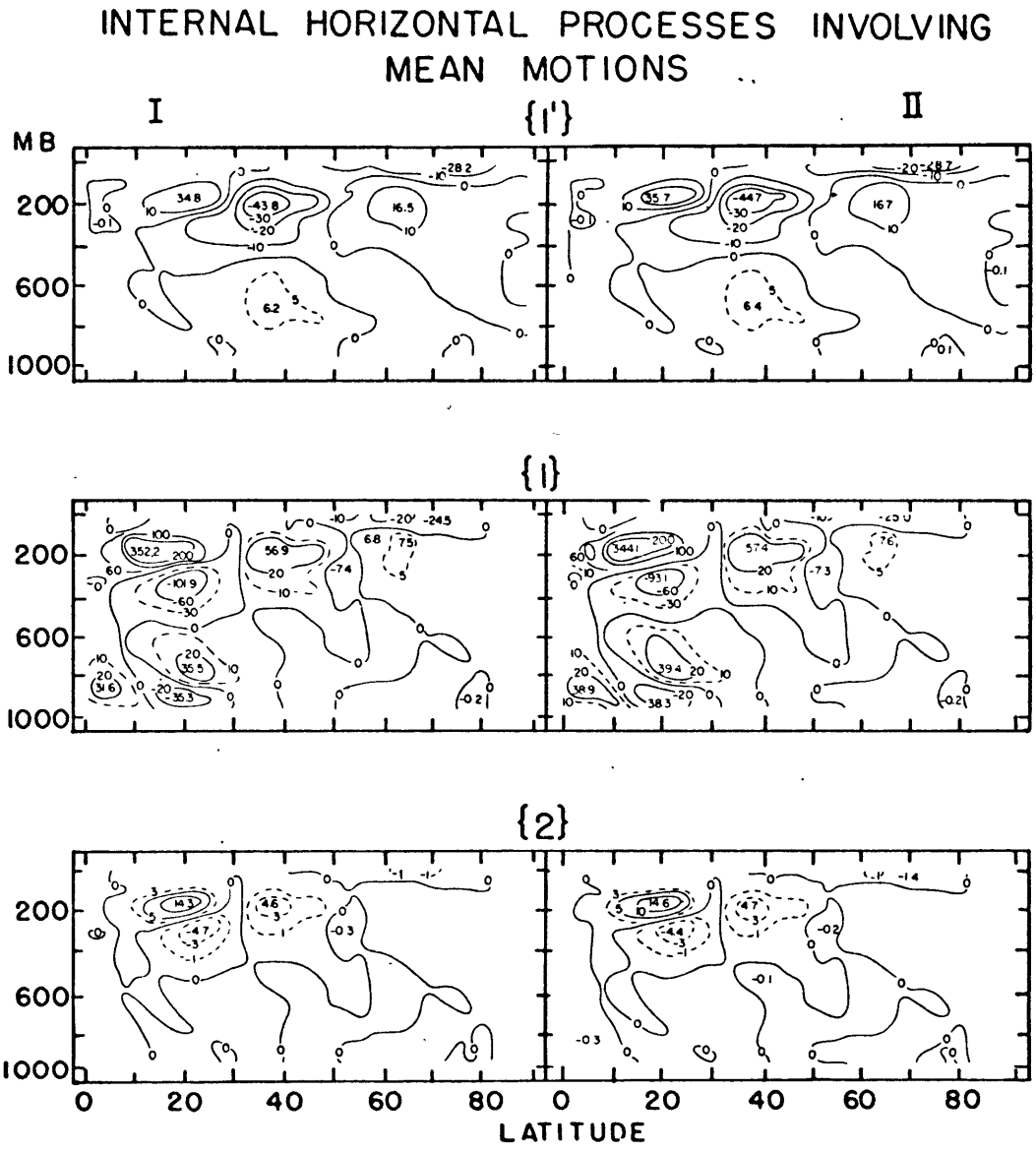

Fig. 5a. These cross sections display the distribution of the integrands of terms {1'} , {1} and {2} and represent the generation of zonal kinetic energy for the internal horizontal processes involving mean motions. The units are 10^6 cm^2 sec^{-1}. The values in column I were calculated from the augmented wind data, while the computations shown in column II were obtained from the original data.

Table 4. Generation of zonal kinetic energy by internal horizontal processes for atmospheric volumes of various depth. Units are 10^{20} ergs sec^{-1}.

1013 mb to	$\{1'\}$		$\{1\}$		$\{2\}$		$\{3'\}$		$\{3''\}$	
	I	II	I	II	I	II	I	II	I	II
913 mb	0.58	0.87	-1.12	-1.46	0	0	0	0	0	0
813 mb	1.69	1.96	0.73	1.28	0	0	0	0.01	0.06	0.01
713 mb	3.02	3.36	4.83	5.91	0.02	0.02	-0.01	-0.01	0.19	0.19
613 mb	3.76	4.18	7.67	9.34	0.04	0.04	-0.01	-0.01	0.43	0.43
513 mb	4.19	4.73	7.81	10.3	0.04	0.05	0.04	0.04	0.86	0.86
413 mb	3.13	3.84	2.61	6.04	-0.07	-0.03	0.22	0.22	1.45	1.45
313 mb	0.06	0.96	-7.96	-3.63	-0.39	-0.32	0.47	0.47	2.45	2.44
213 mb	-1.61	-0.48	21.0	25.9	0.44	0.57	0.15	0.15	4.13	4.12
113 mb	-0.79	0.54	68.9	73.7	2.07	2.23	-0.17	-0.18	5.36	5.34
13 mb	-4.92	-3.73	69.9	74.5	2.05	2.22	-0.23	-0.24	5.67	5.64

allowed to vary by 100 mb increments up to the 13 mb pressure surface. The hemispheric value of $\{1'\}$ is increased by roughly 30 percent through the use of alternate station data. The disparity between the two sets of values is greatest for the volumes extending above 313 mb. Within these volumes, strong winds associated with the mean jet should have their maximum effect in reducing the number of observations at the primary stations.

2. Evaluation of term $\{1\}$:

$$\iint \frac{2\pi a^2}{g} \cos^2\phi (\Omega a \cos\phi)[\bar{v}] \frac{\partial}{a\,\partial\phi}\left\{\frac{[\bar{u}]}{a\cos\phi}\right\} a\,d\phi\,dP$$

Term $\{1\}$ represents the generation of mean zonal kinetic energy through the meridional transport of angular momentum associated with the rotation of the earth, Ω . Because of the large magnitude of $a\Omega\cos\phi$ the above term, as well as the other Ω-terms in equation (5), are sensitive to changes in $[\bar{v}]$ or $[\bar{\omega}]$. The factor $\cos^3\phi$ appearing in these terms, however, nullifies the importance of such effects at high latitudes.

The middle two panels of Fig. 5a depict the distribution of the integrand of $\{1\}$. A decrease has taken place in the positive generation in the upper levels north of the mean jet. A somewhat larger change is noticeable in the tropics, where small changes in $[\bar{v}]$ have filtered south of 30°N and are amplified by the factor $a\Omega\cos^3\phi$.

In Table 4, some changes in the value of $\{1\}$ can also be noticed. With the exception of the lowest layer volume, the positive generation of zonal kinetic energy represented by $\{1\}$ is reduced when the alternate station observations are used.

3. Evaluation of term $\{2\}$:

$$\iint \frac{2\pi a^2}{g} \cos^2\phi\, [\bar{u}][\bar{v}] \frac{\partial}{a\partial\phi}\left\{\frac{[\bar{u}]}{a\cos\phi}\right\} a\,d\phi\,dP$$

The above term represents the generation of mean zonal kinetic energy by the meridional transport of angular momentum associated with the relative rotation $[\bar{u}]$. Since the various factors contained in $\{2\}$ are of relatively small magnitude, changes in $[\bar{v}]$ are not so critical in $\{2\}$ as they are in $\{1\}$.

The meridional distribution of the integrand of $\{2\}$ is presented in the bottom two panels of Fig. 5a. Some minor differences can be noted between the two panels in the upper-level region near 20°N. The values of $\{2\}$ appearing in columns I and II of Table 4 are virtually the same for volumes below 313 mb. For volumes extending above 313 mb, the two sets of values slightly diverge. By substituting for missing data, the hemispheric value of $\{2\}$ is reduced from 2.22 to 2.05 x 10^{20} ergs sec^{-1}.

4. Evaluation of term $\{3'\}$:

$$\iint \frac{2\pi a^2}{g} \cos^2\phi\, [\bar{u}^*\bar{v}^*] \frac{\partial}{a\partial\phi}\left\{\frac{[\bar{u}]}{a\cos\phi}\right\} a\,d\phi\,dP$$

Term $\{3'\}$ represents the generation of mean zonal kinetic energy arising from the meridional transport of angular momentum associated with standing eddies.

The meridional distribution of the integrand of $\{3'\}$ is given in the top two cross sections of Fig. 5b. The area of maximum generation located in the tropical lower stratosphere remains unchanged. This result may be partially due to the fact that the region lies outside the area in which alternate station reports are used. However, a closer comparison between the two panels fails to reveal any noticeable differences even in the more northerly latitudes, where alternate stations do exist. The computed values of $\{3'\}$ in Table 4 also demonstrate little, if any, change as a result of adding substituted data. The stability of $\{3'\}$ is in sharp contrast to the previously discussed terms, whose individual values were similar, but nevertheless did change slightly when alternate station observations were used.

5. Evaluation of term $\{3''\}$:

$$\iint \frac{2\pi a^2}{g} \cos^2\phi \, [\overline{u'v'}] \, \frac{\partial}{a\partial\phi} \left\{ \frac{[\bar{u}]}{a\cos\phi} \right\} a \, d\phi \, dP$$

The integral of term $\{3''\}$ represents the generation of mean zonal kinetic energy arising from the meridional transport of angular momentum associated with transient eddies.

Since the maximum negative viscosity effect associated with transient eddies occurs in a region of strong winds (Fig. 2 and Fig. 3),

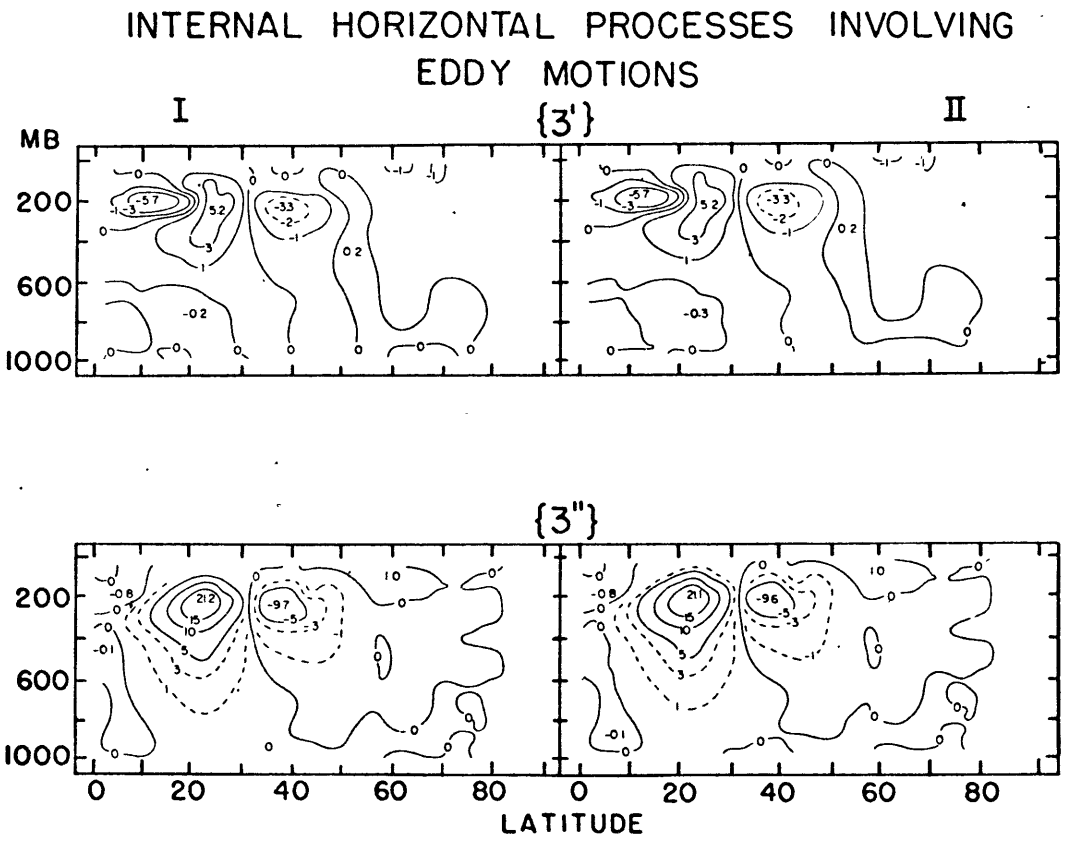

Fig. 5b. Vertical meridional cross sections through the atmosphere showing the distribution of the integrands of terms $\{3'\}$ and $\{3''\}$ for the generation of zonal kinetic energy associated with standing and transient eddies, respectively. The units are 10^6 cm^2 sec^{-1}. The values in column I were obtained from the augmented wind data, while the results shown in column II were calculated from the original data.

one might expect the values of $\{3''\}$ to be readily influenced by missing data due to strong winds. However, from Fig. 5b (bottom two panels), the values appear to be relatively unaffected by the use of substituted observations.

The stability of term $\{3''\}$ is also observed in its values appearing in Table 4. The fact that $\{3''\}$ remained virtually unchanged tends to support previous findings (Starr, Peixoto and Gaut, 1970), which showed $\{3''\}$ to be rather invariant for both observational sampling and small changes in the analysis scheme.

C. Internal vertical processes

1. Evaluation of term $\{4'\}$:

$$\iint \frac{2\pi a^2}{g} \cos^2\phi\,(2\Omega\cos\phi)[\bar{\omega}]\frac{[\bar{u}]}{a\cos\phi}\,a\,d\phi\,dP$$

The quantity $[\bar{\omega}]$ was obtained from $[\bar{v}]$ through mass continuity restrictions. It therefore suffers from the same inaccuracies as discussed with regard to $[\bar{v}]$, and any variation in the terms involving vertical motions should ultimately depend on changes in $[\bar{v}]$.

To provide an insight into the effects of missing data on the vertical internal processes, cross sections through the atmosphere of the meridional distribution of the integrands of $\{4'\}$ and the other internal vertical terms are given in Fig. 6. The top two panels of Fig. 6 picture the distribution of the integrand of $\{4'\}$. While the values are small, some differences exist between the two panels around 30°N.

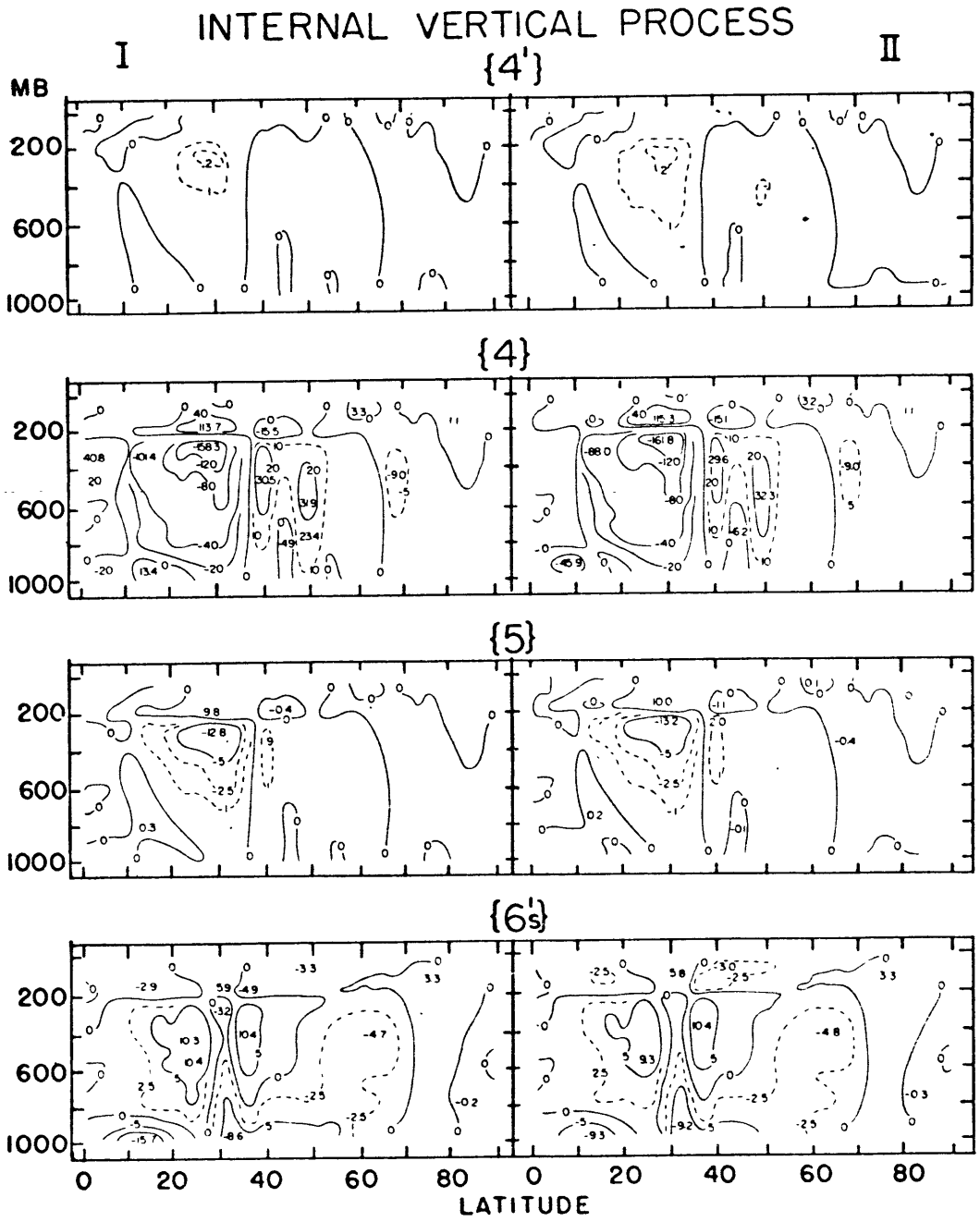

Fig. 6. Meridional cross sections showing the distribution of the integrands of terms {4'} , {4} , {5} and {6's} for the generation of zonal kinetic energy due to internal vertical processes. The units are 10^6 cm^2 sec^{-1}. The values in column I were calculated from the augmented wind data, while the results shown in column II were obtained from the original data.

Table 5 contains the values of $\{4'\}$, as well as the other internal vertical terms, for atmospheric volumes of various depth. The values were obtained in a manner identical to that used in Table 4. The influence of missing data on $\{4'\}$ is of little interest due to the small magnitude of the values.

2. Evaluation of term $\{4\}$:

$$\iint \frac{2\pi a^2}{g} \cos^2\phi \,(-\Omega a \cos\phi)[\bar{\omega}] \frac{\partial}{\partial p}\left\{\frac{[\bar{u}]}{a\cos\phi}\right\} a\,d\phi\,dp$$

The above term represents the generation of mean zonal kinetic energy by the vertical transport of angular momentum associated with the rotation of the earth, Ω .

The two cross sections in Fig. 6 depicting the integrand of $\{4\}$ are surprisingly similar. The only noteworthy difference between the two panels is a minor decrease in the central values in the upper-level region south of 30°N. The values of $\{4\}$ appearing in Table 5 also indicate only a small percentage change, having decreased in absolute magnitude for the calculations involving substituted data. One might have anticipated somewhat larger variations, since $\{4\}$ contains the factor $a\,\Omega\cos\phi$, which should make it fairly sensitive to changes in $[\bar{v}]$.

3. Evaluation of term $\{5\}$:

$$\iint \frac{2\pi a^2}{g} \cos^2\phi\,[\bar{u}][\bar{\omega}] \frac{\partial}{\partial p}\left\{\frac{[\bar{u}]}{a\cos\phi}\right\} a\,d\phi\,dp$$

Table 5. Generation of zonal kinetic energy by internal vertical processes for atmospheric volumes of various depth. Units are 10^{20} ergs sec^{-1}.

1013 mb to	$\{4'\}$		$\{4\}$		$\{5\}$		$\{6's\}$	
	I	II	I	II	I	II	I	II
913 mb	0	0	-1.08	-4.53	0	0.02	-3.84	-3.02
813 mb	0	0	-5.34	-10.0	0	0.01	-5.01	-4.34
713 mb	0	0.01	-13.6	-18.3	-0.04	-0.05	-5.30	-4.80
613 mb	0.01	0.01	-21.7	-26.6	-0.14	-0.17	-5.08	-4.72
513 mb	0.01	0.02	-33.5	-38.9	-0.41	-0.48	-4.34	-4.12
413 mb	0.02	0.03	-47.7	-52.9	-0.90	-1.01	-3.21	-3.08
313 mb	0.04	0.05	-68.7	-73.3	-1.94	-2.09	-1.78	-1.70
213 mb	0.06	0.07	-84.9	-88.9	-3.09	-3.26	-0.76	-0.69
113 mb	0.07	0.08	-76.2	-80.7	-2.33	-2.47	-0.99	-0.95
13 mb	0.07	0.08	-74.3	-78.9	-2.21	-2.35	-1.24	-1.26

Term $\{5\}$ represents the generation of mean zonal kinetic energy by the vertical transport of angular momentum associated with the relative rotation $[\bar{u}]$.

The meridional distribution of the integrand of $\{5\}$ is given in the third row of panels in Fig. 6. The maximum value of $\{5\}$ occurs in conjunction with the mean downward motion associated with the mid-latitude indirect cell. This maximum value is slightly reduced in the calculations using the alternate station reports. From Table 5, the overall effect of substituting for missing data was to inhibit the negative generation of zonal kinetic represented by $\{5\}$. The hemispheric value of $\{5\}$ decreased from -2.35 to -2.21 x 10^{20} ergs sec^{-1} through the use of alternate stations.

4. Evaluation of term $\{6's\}$:

$$\int\int \frac{2\pi a^2}{g} \cos^2\phi \left([\bar{u}^*\bar{\omega}^*] + [\overline{u'\omega'}] + [\bar{\tau}_F]\right) \frac{\partial}{\partial p}\left\{\frac{[\bar{u}]}{a\cos\phi}\right\} a\, d\phi\, dp$$

The generation of mean zonal kinetic energy due to the vertical transport of angular momentum by eddies of all scales (including friction) is represented by $\{6's\}$.

Since the term represents a composite of different scales of vertical motion, it is perhaps important to point out the signficance attached to the sign of $\{6's\}$. Since molecular scale eddies (friction) tend to reduce the kinetic energy of the zonal flow, positive values represent net generation due to the negative viscosity effects of large-scale vertical eddies. On the other hand, negative values represent net negative genera-

tion, which can be ascribed to either large-scale eddies acting in the classical sense, or frictional dissipation, or a combination of both.

The bottom two panels in Fig. 6 represent the distribution of the integrand of $\{6's\}$. Some small differences exist between the two panels in the area of positive generation located in the middle troposphere south of the mean jet. Both the maximum value and the lateral extent of this region have increased for the panel shown in column I. However, the use of additional reports fails to produce any significant variation between the two cross sections, or in the values of $\{6's\}$ presented in Table 5.

D. Vertical boundary processes

1. Evaluation of term $\{7\}$ at $\phi = \phi_1$:

$$\int \frac{2\pi a^2}{g} \cos^2\phi_1 (\Omega a \cos\phi_1)[\bar{v}] \frac{[\bar{u}]}{a\cos\phi_1} dP$$

The above term represents the transport of mean zonal kinetic energy resulting from work done by the stress component associated with the rotation of the earth, Ω , acting across the latitude wall at ϕ_1 .

The meridional distribution of the integrands of the vertical boundary terms in equation (5) are shown in Fig. 7. The units are 10^{14} cm^3 sec^{-1}. Positive regions in the cross sections represent the northward transport of zonal kinetic energy by Reynolds stresses, acting across free boundary surfaces. In the two panels depicting the integrand of $\{7\}$, the transport of zonal kinetic energy between 30°N and 40°N is of

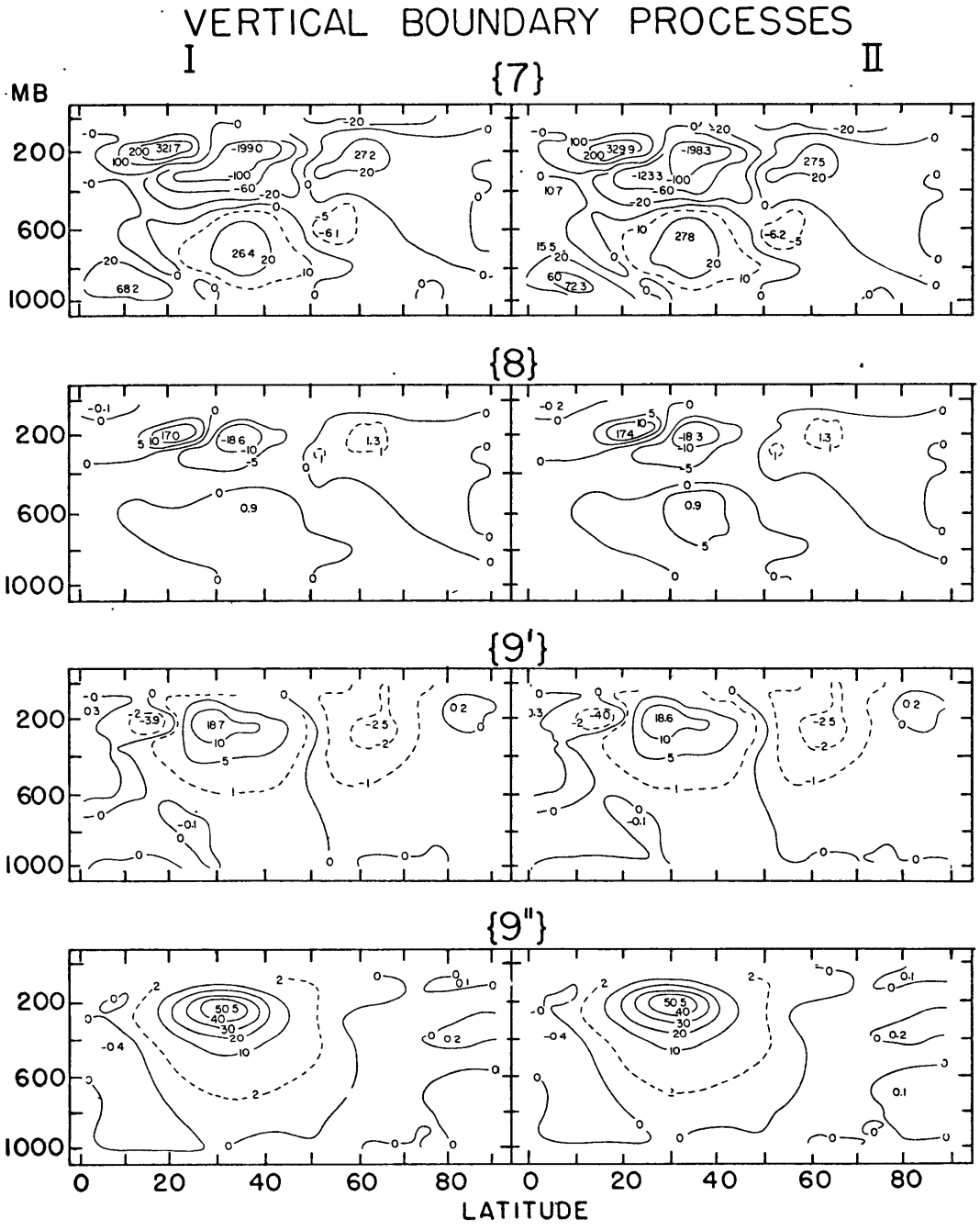

Fig. 7. These cross sections show the distribution of the integrands of the terms indicated and represent the transport of zonal kinetic energy due to vertical boundary processes. The units are 10^{14} cm^3 sec^{-1}. The results in column I were obtained from the augmented wind data, while the values in column II were computed from the original data.

particular interest. The number of substituted reports should be a maximum in this region, and it is within these middle latitudes that strong winds and severe weather should have their optimum effect in reducing the number of reports. The area of northward transport shows a small decrease in value, while the upper-level southward transport is slightly increased by using alternate station reports.

Table 6 contains the values of the integrands pictured in Fig. 7. The units are 10^{20} ergs sec^{-1}. The integrals are computed at every two degrees of latitude. The vertical profiles of the integrals are plotted in Fig. 8. (Note that the vertical scale for $\{7\}$ is an order of magnitude larger than that of the other terms pictured in Fig. 8.) The values of $\{7\}$ in Table 6 are fairly consistent, though again, some small changes can be detected between the two sets of computations. The transport of energy into the mean jet in the region between 30^{o}N and 40^{o}N has been somewhat enhanced through substituting for missing data. South of the jet, where presumably the variations are due to smoothing in the analysis, the net northward energy transport has slightly decreased.

2. Evaluation of term $\{8\}$ at $\phi = \phi_1$:

$$\int \frac{2\pi a^2}{g} \cos^2\phi_1 \, [\bar{u}][\bar{v}] \frac{[\bar{u}]}{a\cos\phi_1} \, dP$$

Term $\{8\}$ represents the transport of mean zonal kinetic energy resulting from work done by the stress component associated with the relative rotation $[\bar{u}]$, acting across the latitude wall at ϕ_1 .

Table 6. Transport of zonal kinetic energy across various latitude walls by vertical boundary processes. Units are 10^{20} ergs sec^{-1}.

Lat. (°N)	{7}		{8}		{9'}		{9''}	
	I	II	I	II	I	II	I	II
0	3.65	4.66	-0.03	-0.04	0.07	0.06	0.49	0.05
2	7.90	8.55	-0.06	-0.07	0.06	0.05	0	0
4	10.8	12.4	-0.09	-0.10	0.05	0.03	-0.05	-0.05
6	14.4	15.8	-0.09	-0.10	0	-0.02	-0.09	-0.09
8	20.2	21.3	-0.04	-0.04	-0.10	-0.12	-0.07	-0.06
10	27.4	28.4	0.11	0.11	-0.23	-0.24	0.10	0.11
12	30.8	32.1	0.35	0.36	-0.29	-0.29	0.54	0.55
14	31.3	33.4	0.66	0.67	-0.24	-0.24	1.32	1.33
16	29.9	33.1	0.94	0.98	-0.05	-0.05	2.46	2.47
18	26.3	30.6	1.15	1.23	0.32	0.32	3.99	3.99
20	19.4	24.5	1.05	1.19	0.88	0.88	5.75	5.74
22	10.5	15.9	0.66	0.86	1.84	1.83	7.69	7.69
24	3.83	8.92	-0.26	0.50	3.12	3.11	9.57	9.56
26	-3.47	0.86	-0.35	-0.11	4.04	4.04	11.0	11.0
28	-12.6	-8.90	-1.19	-0.97	4.36	4.36	12.2	12.2
30	-22.2	-19.3	-2.12	-1.93	3.97	3.98	12.6	12.6
32	-30.8	-28.8	-2.96	-2.83	3.16	3.18	12.3	12.3
34	-33.5	-32.3	-3.17	-3.10	2.75	2.78	11.2	11.2
36	-30.9	-30.4	-2.83	-2.81	2.77	2.80	9.62	9.62
38	-25.4	-25.4	-2.24	-2.24	2.60	2.63	7.94	7.95
40	-18.6	-18.8	-1.54	-1.56	2.12	2.14	6.13	6.13

Table 6. (continued)

Lat. (°N)	{7}		{8}		{9'}		{9''}	
	I	II	I	II	I	II	I	II
42	-14.3	-14.7	-1.12	-1.14	1.73	1.75	4.61	4.61
44	-12.1	-12.6	-0.88	-0.90	1.34	1.36	3.47	3.47
46	-9.43	-9.86	-0.64	-0.63	0.80	0.81	2.50	2.50
48	-5.21	-5.60	-0.30	-0.31	0.25	0.25	1.78	1.78
50	-1.06	-1.39	-0.05	-0.06	-0.16	-0.16	1.30	1.30
52	0.92	0.65	0.06	0.05	-0.46	-0.46	0.93	0.93
54	1.35	1.15	0.08	0.08	-0.73	-0.73	0.64	0.64
56	1.77	1.65	0.11	0.10	-0.91	-0.91	0.39	0.39
58	2.56	2.56	0.15	0.15	-0.99	-0.99	0.13	0.13
60	3.10	3.18	0.17	0.18	-1.08	-1.08	-0.06	-0.06
62	3.30	3.39	0.18	0.19	-1.11	-1.11	-0.15	-0.15
64	3.28	3.35	0.18	0.18	-1.12	-1.12	-0.20	-0.20
66	2.83	2.88	0.16	0.16	-1.05	-1.05	-0.23	-0.23
68	1.74	1.80	0.09	0.10	-0.91	-0.91	-0.27	-0.27
70	0.55	0.61	-0.01	0.01	-0.77	-0.77	-0.29	-0.29
72	0.14	0.21	-0.02	-0.02	-0.56	-0.57	-0.25	-0.25
74	0.01	0.01	-0.03	-0.03	-0.34	-0.34	-0.17	-0.17
76	-0.16	-0.11	-0.05	-0.04	-0.18	-0.18	-0.10	-0.10
78	-0.19	-0.16	-0.04	-0.04	-0.08	-0.08	0.04	-0.04
80	-0.18	-0.17	-0.04	-0.04	-0.08	-0.01	0	0
82	-0.09	-0.09	-0.02	-0.02	-0.02	0	0	0
84	-0.02	-0.02	-0.01	-0.01	0	0	0	0
86	0	-0.01	0	0	0	0	0	0
88	0	0	0	0	0	0	0	0

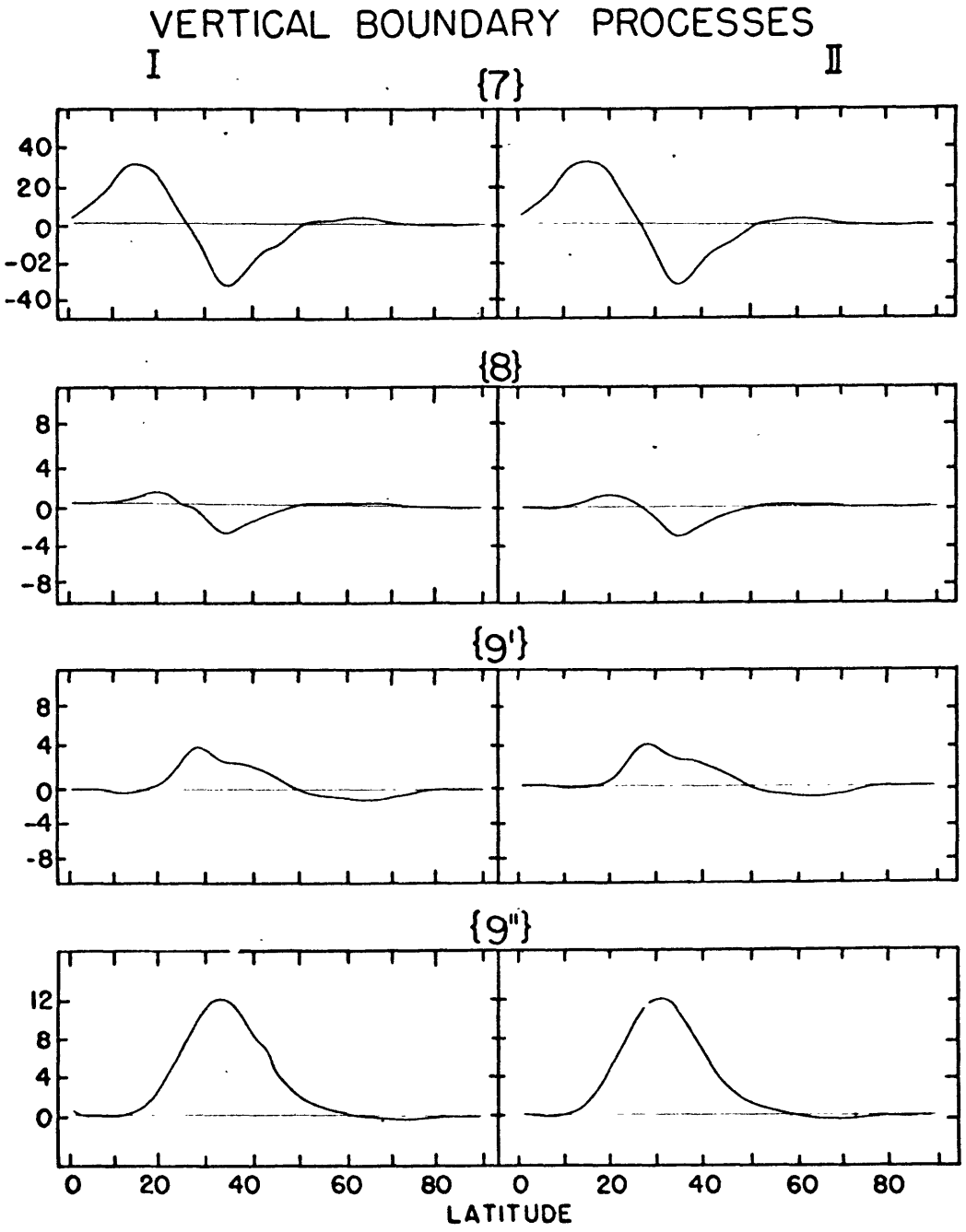

Fig. 8. Meridional profiles of terms {7} , {8} , {9'} and {9"} representing the transport of zonal kinetic energy across various latitude walls. The units are 10^{20} ergs sec^{-1}. The values in column I were calculated from the augmented wind data, while the results shown in column II were obtained from the original data.

The dependence of $\{8\}$ upon the quantity $[\bar{u}]^2$ makes the term sensitive to variations in $[\bar{v}]$ which occur in the vicinity of the mean jet. From Fig. 7, we can see that a small increase has taken place in the amount of energy being fed southward into the jet. This change is also reflected in the values of $\{8\}$ shown in Table 6.

3. Evaluation of term $\{9'\}$ at $\phi = \phi_1$:

$$\int \frac{2\pi a^2}{g} \cos^2\phi_1 \, [\bar{u}^*\bar{v}^*] \frac{[\bar{u}]}{a\cos\phi_1} \, dP$$

The above term represents the mean zonal kinetic energy transport resulting from the work done by the stress component associated with the standing eddy motions, acting across the latitude wall at ϕ_1 .

Meridional cross sections displaying the integrand of $\{9'\}$ are given in the third row of panels in Fig. 7. The two panels for $\{9'\}$ are virtually identical. The stability of $\{9'\}$ is further demonstrated in the meridional profiles shown in Fig. 8.

4. Evaluation of term $\{9''\}$ at $\phi = \phi_1$:

$$\int \frac{2\pi a^2}{g} \cos^2\phi_1 \, [\overline{u'v'}] \frac{[\bar{u}]}{a\cos\phi_1} \, dP$$

Term $\{9''\}$ represents the transport of mean zonal kinetic energy resulting from the work done by the stress component associated with transient eddy motions, acting across the latitude wall at ϕ_1 .

The use of additional data has no appreciable influence on the values of the integrand $\{9''\}$ pictured in Fig. 7. The values of $\{9''\}$ in

Table 6 and Fig. 8 are also relatively unaffected by using the substituted observations.

E. Horizontal boundary processes

1. Evaluation of term $\{10\}$ at $p = p_1$:

$$-\int \frac{2\pi a^2}{g} \cos^2\phi \,(\Omega a \cos\phi)[\bar{\omega}] \frac{[\bar{u}]}{a\cos\phi}\, a\, d\phi$$

Term $\{10\}$ represents the transport of mean zonal kinetic energy resulting from the work done by the stress component associated with the rotation of the earth, Ω , acting across the pressure surface at p_1 . As with the previously discussed Ω-terms, $\{10\}$ is generally large and should be sensitive to variations in $[\bar{\omega}]$.

To aid in studying the effects of missing data on the horizontal boundary processes, the meridional distribution of the integrands of terms $\{10\}$, $\{11\}$ and $\{12\text{'s}\}$ are pictured in Fig. 9. The units are 10^{12} ergs cm^{-1} sec^{-1}. Positive regions in the cross sections represent the net downward transport of mean zonal kinetic energy by Reynolds stresses acting across free boundary surfaces. The two panels displaying the integrand of $\{10\}$ show a small difference in the central value near 28°N. The downward flux of zonal kinetic energy in this region is increases from 58.0 to 60.3 by using alternate station observations.

Table 7 contains the values of the horizontal integrals of the quantities shown in Fig. 9. The units are 10^{20} ergs sec^{-1}. The values are computed at 50 mb intervals beginning at the 913 mb level and going

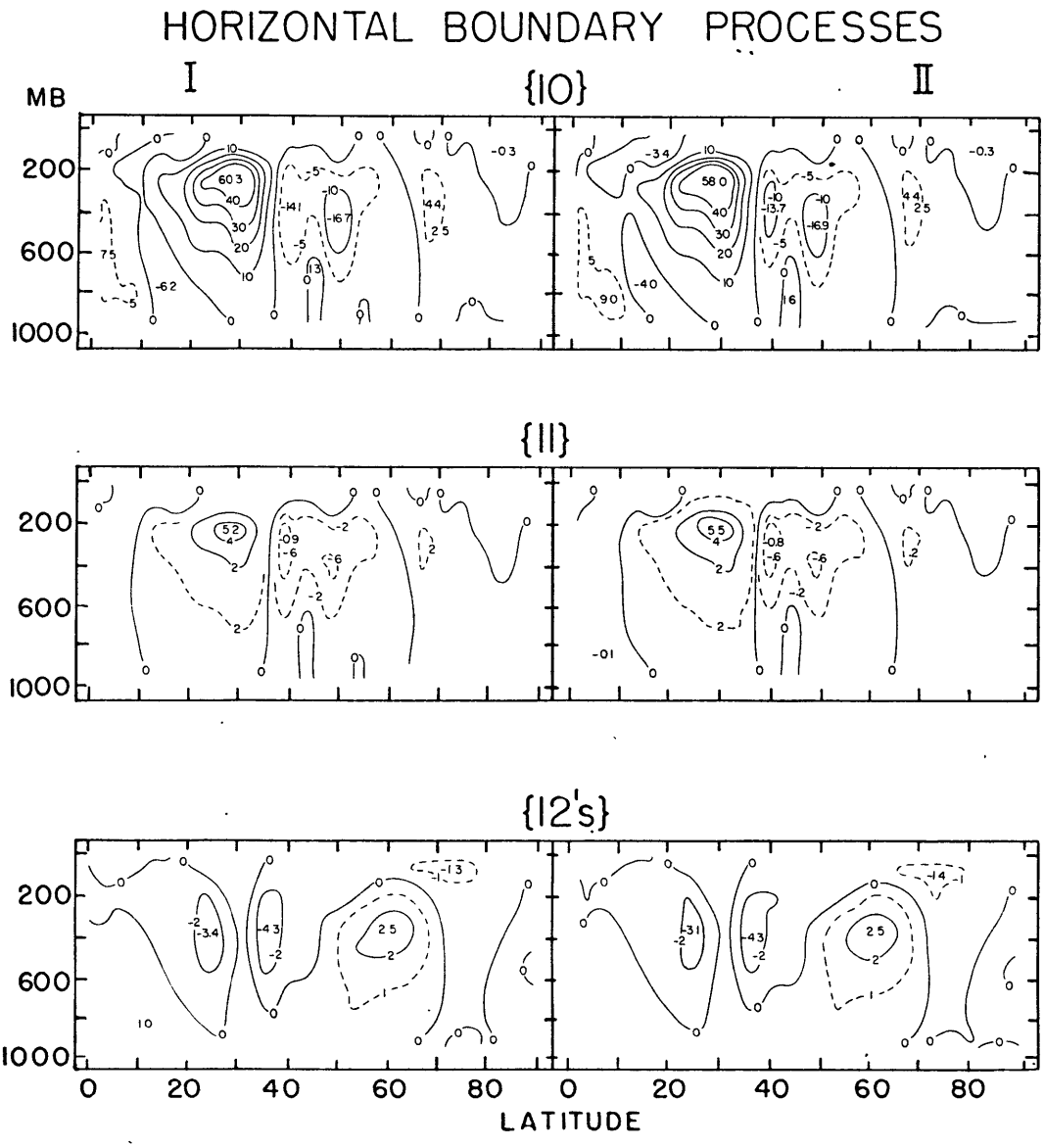

Fig. 9. The above cross sections depict the distribution of the integrands of terms {10}, {11} and {12's} and represent the transport of zonal kinetic energy due to horizontal boundary processes. The units are 10^{12} ergs cm^{-1} sec^{-2}. The values in column I were computed using alternate station reports in place of missing primary station reports whenever possible. These values are to be compared with the results in column II, which were obtained using the original station reports.

Table 7. Transport of zonal kinetic energy across various pressure surfaces by horizontal boundary processes. Units are 10^{20} ergs sec^{-1}.

Pressure (mb)	{10} I	{10} II	{11} I	{11} II	{12's} I	{12's} II
13	—	—	—	—	—	—
63	2.52	2.66	0.11	0.12	-2.12	-2.22
113	9.21	9.35	0.60	0.63	-3.27	-3.44
163	27.9	27.9	2.28	2.63	-3.44	-3.60
213	57.8	57.7	4.88	5.01	-4.27	-4.36
263	74.8	75.1	5.72	5.89	-4.30	-4.31
313	69.9	70.8	4.48	4.65	-3.30	-3.21
363	57.7	58.5	3.08	3.25	-2.64	-2.47
413	43.6	46.1	2.04	2.19	-2.28	-2.05
463	33.2	36.1	1.32	1.45	-1.76	-1.47
513	25.6	28.9	0.86	0.98	-0.95	-0.64
563	19.4	22.9	0.53	0.62	-0.02	0.33
613	13.9	17.6	0.28	0.34	0.91	1.25
663	10.5	14.3	0.15	0.19	1.64	1.96
713	8.51	12.5	0.09	0.11	2.26	2.57
763	6.08	10.4	0.04	0.05	2.89	3.18
813	3.85	8.44	0.01	-0.01	3.40	3.62
863	2.63	7.43	-0.01	-0.04	3.64	3.77
913	1.42	5.73	-0.01	-0.04	3.39	3.48
963	0.30	2.44	0	-0.01	2.15	2.58
1013	—	—	—	—	—	—

up to the 63 mb pressure surface. The profiles of the integrals are plotted in Fig. 10. Comparing the two sets of values for $\{10\}$ in Table 7, one can see that the spread is greatest in the middle levels. Surprisingly, the two values are quite close around the level of the mean jet, where any light wind bias would be at a maximum.

2. Evaluation of term $\{11\}$ at $p = p_1$:

$$-\int \frac{2\pi a^2}{g} \cos^2\phi\, [\bar{u}][\bar{\omega}] \frac{[\bar{u}]}{a\cos\phi}\, a\, d\phi$$

The transport of mean zonal kinetic energy resulting from the work done by the stress component associated with the relative motion $[\bar{u}]$, acting across the pressure surface at p_1 .

The middle two panels in Fig. 9 represent the distribution of the integrand of $\{11\}$. The values appear relatively unaffected by using substituted reports. Some very minor changes have taken place in $\{11\}$, when one considers the profiles shown in Fig. 10 (note the difference in horizontal scale between $\{10\}$ and the other terms presented in the figure). The use of additional data has resulted in a slight decrease in the downward flux of zonal kinetic energy at all levels. The maximum difference between the two sets of computations takes place near the level of the mean jet, where any effect from missing data is amplified by the factor $[\bar{u}]^2$ appearing in $\{11\}$.

3. Evaluation of term $\{12's\}$ at $p = p_1$:

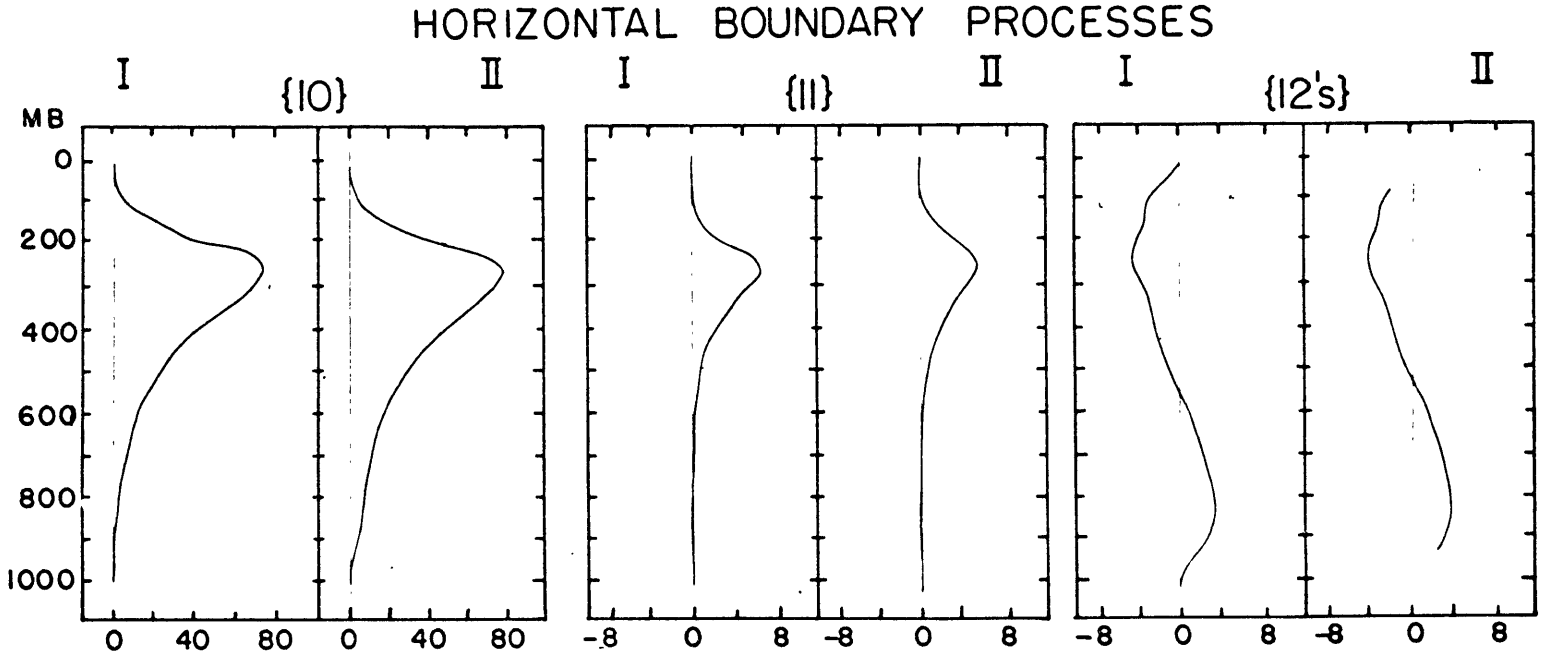

Fig. 10. Vertical profiles of terms $\{10\}$, $\{11\}$ and $\{12's\}$ depicting the transport of zonal kinetic energy across various pressure surfaces. The units are 10^{20} ergs sec^{-1}. The values in column I were calculated from the augmented wind data, while the results shown in column II were obtained from the original data.

$$-\int \frac{2\pi a^2}{g} \cos^2\phi \left([\bar{u}^* \bar{\omega}^*] + [\overline{u'\omega'}] + [\bar{\tau}_F] \right) \frac{[\bar{u}]}{a\cos\phi} a\,d\phi$$

Term {12's} represents the transport of mean zonal kinetic energy resulting from work done by the stress component associated with all scales of vertical eddies (including friction), acting across the pressure surface at p_1 .

The two panels depicting the meridional distribution of the integrand of {12's} are practically identical. Viewing the values of {12's} plotted in Fig. 10 and displayed in Table 7, some slight changes have taken place using the substituted data. Below 613 mb, the net downward flux of zonal kinetic energy has decreased, while in the region above that level, the net upward transport shows a comparable increase.

F. Other considerations

In the previous sections, the terms appearing in both the traditional and the symmetrical forms of the zonal kinetic energy equation were discussed individually with regard to the effects of missing data. In this section we shall deal with the effects of missing data as they apply to the net zonal kinetic energy balance in atmospheric volumes of various depth.

Since the kinetic energy of the zonal flow should be essentially conserved in the long-term average, the sums of the respective terms in both forms of the zonal kinetic energy equation should theoretically equal zero. This condition is imposed in the calculations by using mass-continuity

conditions and by incorporating the frictional dissipation with the effects of vertical eddies in terms $\{6's\}$ and $\{12's\}$.

As a result of the smooth-earth approximation, the torque exerted upon the atmosphere by the pressure differential across mountain ranges is neglected in both the traditional and symmetrical forms of the energy equation (see Starr and Gaut, 1969). The omission of this term can then lead to systematic errors in the net zonal kinetic energy balance. These errors are reduced by utilizing the mean pressure differential across mountain barriers, as computed by White (1949).

Table 8 contains the results of balancing the individual term appearing in the traditional form of the zonal kinetic energy equation, with the mountain torque correction included. The units are 10^{20} ergs sec^{-1}. The values in column I are computed from the modified data, and are to be compared with the results in column II, which are computed from the original station reports. The values of the vertical boundary terms($\{8\}$, $\{9'\}$ and $\{9''\}$) represent the flux of zonal kinetic energy through a vertical wall of variable height placed at the equator. The values of the remaining terms have been presented previously (Tables 4, 5, and 7) and are included here simply for completeness.

The sums of the terms for both sets of calculations appear in the row labeled residual. Because of the imposed continuity restriction, the magnitude of these residuals is more representative of the accuracy of the computations than the quality of the data. Nevertheless, some

Table 8. Mean zonal kinetic energy balance for atmospheric volumes of various depth. Units are 10^{20} ergs sec^{-1}.

1013 mb to	913 mb		813 mb		713 mb		613 mb		513 mb	
	I	II	I	II	I	II	I	II	I	II
{1'}	0.58	0.87	1.69	1.96	3.02	3.36	3.76	4.18	4.19	4.73
{2}	0	0	0	0	0.02	0.02	0.04	0.04	0.04	0.05
{3'}	0	0	0	0.01	-0.01	-0.01	-0.01	-0.01	0.04	0.04
{3''}	0	0	0.06	0.01	0.19	0.19	0.43	0.43	0.86	0.86
{4'}	0	0	0	0	0	0.01	0.01	0.01	0.01	0.01
{5}	0	0.02	0	0.01	-0.04	-0.05	-0.14	-0.17	-0.41	-0.48
{6's}	-3.84	-3.02	-5.01	-4.34	-5.30	-4.80	-5.08	-4.72	-4.34	-4.12
{8}	-0.01	0	-0.02	-0.01	-0.03	-0.03	-0.03	-0.03	-0.03	-0.03
{9'}	0.01	0	0.03	0.01	0.03	0.03	0.03	0.03	0.03	0.03
{9''}	0	0	0.01	0	0.02	0	0.02	0	0.02	0
{11}	-0.01	-0.04	0.01	-0.01	0.09	0.11	0.28	0.34	0.86	0.98
{12's}	3.39	3.48	3.40	3.62	2.26	2.57	0.91	1.25	-0.95	-0.64
mountain torque	-0.14		-0.14		-0.14		-0.14		-0.14	
residual	-0.02	1.17	0.16	1.18	0.23	1.28	0.21	1.24	0.30	1.33

Table 8. (continued)

1013 mb to	413 mb		313 mb		213 mb		113 mb		13 mb	
	I	II	I	II	I	II	I	II	I	II
{1'}	3.13	3.84	0.06	0.96	-1.61	-0.48	-0.79	0.54	-4.92	-3.73
{2}	-0.07	-0.03	-0.39	-0.32	0.44	0.57	2.07	2.23	2.05	2.22
{3'}	0.22	0.22	0.47	0.47	0.15	0.15	-0.17	-0.18	-0.23	-0.24
{3"}	1.45	1.45	2.45	2.44	4.13	4.12	5.36	5.34	5.67	5.64
{4'}	0.02	0.03	0.04	0.05	0.06	0.07	0.07	0.08	0.07	0.08
{5}	-0.90	-1.01	-1.94	-2.09	-3.09	-3.26	-2.33	-2.47	-2.21	-2.35
{6's}	-3.21	-3.08	-1.78	-1.70	-0.76	-0.69	-0.99	-0.95	-1.24	-1.26
{8}	-0.03	-0.03	-0.03	-0.03	-0.03	-0.03	-0.03	-0.03	-0.04	-0.03
{9'}	0.03	0.03	0.04	0.04	0.05	0.03	0.07	0.05	0.06	0.07
{9"}	0	-0.01	-0.02	-0.02	-0.02	-0.01	0.01	0	0.05	0.06
{11}	2.04	2.19	4.48	4.65	4.88	5.01	0.60	0.63	—	—
{12's}	-2.28	-2.05	-3.30	-3.21	-4.27	-4.36	-3.27	-3.44	—	—
mountain torque	-0.14		-0.14		-0.14		-0.14		-0.14	
residual	0.43	1.43	0.07	1.10	0.48	0.99	0.60	1.69	-0.71	0.29

interesting similarities and differences exist between the two sets of values.

The largest spread between the two residuals occurs not in the vicinity of the mean jet, or even in the upper-levels, but in the lowest layer volume between 1013 mb and 913 mb, where the two values differ by 1.19. Since the residuals are for cumulative layers, this value then accounts for most of the difference observed between the values in the volumes extending above the 913 mb level. Both residuals behave poorly, when the volume contained in the topmost 100 mbs is included in the calculations. Similar results have been noted in previous computations involving the full 799 station network (Rosen, 1970) and have been ascribed to poor data and also the imposed mass-continuity restriction. (The latter artificially forces the horizontal boundary processes to zero at the 13 mb pressure surface, which is taken to be the top of the atmosphere.) However, since the input of substituted reports is greatest at high altitudes (Table 2), it appears that missing data by itself has little influence on the residual near the upper-level boundary.

From the viewpoint of residuals, the net effect of using substituted data at the various levels is somewhat discouraging. A hemispheric value of -0.71 occurs from using the modified data, while the orignal data yields a value of only +0.29.

Briefly comparing the hemispheric values of some of the individual terms in the table, we can see that the largest percentage change occurs in $\{1'\}$, while the terms involving horizontal eddies ($\{3'\}$, $\{3''\}$,

$\{9'\}$ and $\{9''\}$) remain virtually unaffected. The vertical eddy terms, $\{6's\}$ and $\{12's\}$, are also fairly consistent, which is rather surprising since they are obtained indirectly from values of $[\bar{v}]$. Finally there is a tendency for the changes in terms $\{2\}$ and $\{5\}$ to cancel, which should perhaps be expected, since $[\bar{v}]$ and $[\overline{\omega}]$ are related to each other through mass-continuity.

CHAPTER VI. CONCLUSION

A. General remarks and recommendations for further research

It was suggested in the introduction that strong winds and/or severe weather could influence the values of $[\bar{v}]$ by reducing the number of wind measurements possessing northerly components. We found the vertical averages of $[\bar{v}]$ to be somewhat less negative in the middle latitudes (Fig. 4 and Table 3), but overall the use of substituted reports failed to reveal any systematic differences between the two cross sections of $[\bar{v}]$ in Fig. 2. Indeed, the two panels are so similar, that it causes one to question the effectiveness of substituting alternate station reports to compensate for the missing data.

The effects of missing data are admittedly diluted, since only 59 of the 206 stations possess alternate station clusters. Of greater significance, however, is the percent of missing primary station observations compensated for at the various levels by the use of alternate station reports. As shown in Table 2, the procedure is most effective in the middle levels, moderately successful in the upper levels, but fairly poor in the lowest levels. The small number of observations available below 900 mbs is undoubtedly the result of many stations being located above that level. In the upper levels when the wind is exceptionally strong over a primary station, the flow on either side may be strong enough at times to also cause the alternate station report to be missing. Thus, the substitution

procedure may not be entirely effective in the case of missing data due to strong winds. This suggestion is supported by the fact that no noticeable increase occurred in the mean zonal velocity, $[\bar{u}]$, and that the greatest change in individual terms generally occurred in regions located away from the mean jet. This problem cannot be satisfactorily answered here, since the prese nt investigation can not actually resolve the different causes for missing data. Repeating the calculations for a season when the winds are not so strong, for example fall, might improve the wind statistics in the upper levels and provide some insight into this problem. An even better procedure, which tests only for a light wind bias, would be to eliminate 10 percent of the strongest winds at each station, say at the 200 or 300 mb levels.

While no systematic bias was detected in the values of $[\bar{v}]$, there was a tendency for the for the terms computed directly from $[\bar{v}]$ ($\{1'\}$, $\{1\}$, $\{2\}$, $\{7\}$, and $\{8\}$) to become more negative, or less positive, when the modified values of $[\bar{v}]$ were used. This somewhat unexpected result could be due to the biased sampling of the wind field brought about by the asymmetry in the primary station distribution. Furthermore, there are undoubtedly some errors introduced in the lower levels, where local topographic influences can render the substituted observation unrepresentative of conditions at the primary station. For high latitude stations, using a maximum distrance of 400 km between a primary and alternate station may also introduce unrepresentative data .

The fact that the vertical averages of $[\bar{v}]$ in this investigation and in the observational studies mentioned earlier (e. g., Starr, Peixoto and Sims, 1970; Tucker, 1959; and Palmen and Vuorela, 1963) were not zero demonstrates the difficulties in obtaining accurate estimates of $[\bar{v}]$. It may be impossible to produce significantly better values of $[\bar{v}]$ without a much more dense station network than is presently feasible, or even practical in the near future. One way to by-pass the uncertainties associated with $[\bar{v}]$ is to calculate it indirectly from momentum and mass-balance considerations (e. g., Gilman, 1965 and Holopainen, 1967). In spite of losing some of the luster that is associated with a purely observational study, it would appear profitable to repeat the calculations using indirect values of $[\bar{v}]$.

In both calculations, the residuals behaved poorly near the upper boundary implying a need for further study in this area. Part of the problem lies with the fact that reliable estimates of vertical motion using independent methods are not yet possible. The effect of the imposed continuity restriction on vertical processes and consequently on the zonal kinetic energy balance is yet to be completely resolved.

The transport of zonal kinetic energy upward to drive the stratospheric refrigerator is another interesting point for further study. A comparison between indirectly measured zonal kinetic energy transports and transports calculated using adiabatic $[\bar{\omega}]$'s could be used to isolate and study the effects of nonadiabatic processes associated with the

tropospheric heat engine.

Alternate station data could do little to improve the sparse data regions over oceans. The use of satellite-viewed cloud patterns and features to infer the circulation in these data sparse regions is promising. Macdonald (1968, 1969) has obtained rough estimates of the mean wind field and the mean momentum flux by following the daily movements of cyclones and anticyclones from satellite photographs. Studies by others (e. g., Shenk and Kreins, 1970), using cloud movements, yield upper level wind statistics that appear comparable to conventional measurements. To utilize any sort of satellite data in our five year study, however, it will probably be necessary to collect another five years of data, since the operational use of satellites was limited during the original five year period (May 1958 to April 1963).

B. Summary of conclusions

The fact that both set of calculations yield similar results is encouraging. An adjustment of approximately three to five percent in the total number of missing reports failed to detect any systematic errors in the observed mean wind fields. It was found that the terms involving horizontal eddy motions were the most stable, while the greatest percentage change occurred in the value of the Coriolis term. Even the so-called Ω-terms did not differ appreciably. In short, the missing data had

only a marginal influence on the quantitative results.

Our investigation seems to indicate that even if better methods are found to improve the quantity of upper level reports at individual observation sites, that such methods would act to refine our existing knowledge of the zonal kinetic energy balance, rather than produce drastically different results.

Table 9. A complete station listing. Alternate stations are indented.

1 Walker sequence number	2 W.M.O. block and station number	3 degrees latitude	4 degrees longitude
003	01028	74.52	-19.02
100	21007	78.07	-14.22
010	02077	59.35	-17.95
013	02963	60.82	-23.48
007	01324	60.20	-11.08
011	02084	57.72	-11.78
016	03026	58.22	6.33
015	02005	60.13	1.17
018	03171	56.38	2.88
034	06011	62.05	6.76
025	03953	51.93	10.25
022	03808	50.22	5.32
023	03917	54.65	6.22
027	04202	76.52	68.84
028	04220	68.70	52.87
029	04270	61.18	45.42
030	04310	81.60	16.67
001	01005	78.04	13.38
032	04340	70.42	21.97
045	07510	44.85	.70
044	07354	48.65	-1.72
048	08159	41.68	1.07
046	07645	43.87	-4.40
051	08495	36.15	5.35
054	08536	38.77	9.15
052	08509	38.75	27.09
058	10202	53.37	-7.22
056	10035	54.53	-9.55
037	06260	52.10	-5.18
059	10338	52.47	-9.70
075	13130	45.82	-16.03
081	16604	46.03	-13.03
077	13334	43.52	-16.43
076	13276	44.78	-20.53
074	12843	47.43	-19.18
087	16560	39.25	-9.05
084	16242	41.80	-12.33

1	2	3	4
090	16716	37.90	-23.73
094	17220	38.40	-27.17
089	16622	40.52	-22.97
096	17606	35.15	-33.28
295	40007	36.18	-37.21
097	20046	80.62	-58.05
098	20047	80.45	-52.80
099	20069	79.50	-76.98
105	20674	73.18	-80.23
104	20667	73.18	-70.04
124	23074	69.40	-86.17
111	21647	73.50	-143.23
108	21358	76.15	-152.84
109	21432	76.00	-137.90
118	22217	67.13	-32.43
119	22522	64.98	-34.78
012	02836	67.37	-26.65
116	23552	68.97	-33.05
136	23955	60.43	-77.87
191	29231	58.30	-83.90
131	23552	64.92	-77.82
142	24688	63.27	-143.15
145	24793	62.70	-149.10
144	24790	61.80	-148.80
147	24908	60.33	-102.27
192	29282	58.42	-97.40
146	24817	61.27	-108.02
140	24507	64.17	-100.07
148	24944	60.40	-120.42
212	31004	58.62	-125.37
141	24621	63.77	-121.62
155	25551	64.68	-170.42
157	25594	64.43	-170.23
153	25299	66.17	-169.83
176	27196	58.65	-49.62
132	23804	61.67	-50.85
178	27595	55.58	-49.18
184	28225	58.02	-56.30
210	309538	50.37	-108.75
203	30635	53.43	-108.98
209	30758	52.05	-113.48
207	30710	52.27	-104.35
323	44292	47.43	-106.93

1	2	3	4
219	31538	50.07	-132.13
222	31735	48.52	-135.17
218	31510	50.27	-127.50
221	31707	47.73	-132.93
216	31329	53.07	-132.93
226	31960	43.12	-131.90
407	54292	42.90	-129.52
224	31873	45.87	-133.73
230	32165	44.02	-145.82
337	47420	43.33	-145.58
335	47401	45.42	-141.68
336	47420	43.05	-141.33
233	32217	50.00	-155.38
234	32387	56.32	-160.83
235	32540	52.97	-158.75
236	32618	55.20	-165.98
240	33345	50.40	-30.45
238	33036	52.03	-29.18
239	33317	50.17	-27.05
244	33791	47.93	-33.33
261	35229	50.28	-57.15
260	35121	51.75	-55.10
267	35796	46.90	-75.00
264	35394	49.80	-73.14
269	36096	51.67	-94.38
198	29865	53.75	-91.40
278	37789	40.13	-44.47
277	37549	41.68	-44.95
279	37860	41.00	-49.00
280	37985	38.73	-48.83
291	38836	38.58	-68.78
293	38954	37.50	-71.50
286	38457	41.27	-69.27
292	38880	37.97	-58.33
290	38750	37.47	-53.97
294	38989	36.06	-62.72
297	40427	26.27	-50.62
298	42182	28.58	-45.02
307	42182	28.58	-77.20
314	42809	22.82	-88.45
315	42867	21.10	-79.85
317	43003	19.12	-72.85
319	43279	13.00	-80.18
326	45004	22.32	-114.17

1	2	3	4
334	47187	33.17	-126.20
333	47132	36.27	-127.28
347	47807	33.57	-130.35
340	47590	38.27	-140.90
339	47582	39.72	-140.10
342	47646	36.05	-140.13
341	47600	37.38	-136.90
350	47931	26.35	-127.75
351	47963	30.48	-140.30
343	47678	33.12	-139.78
352	48327	18.78	-98.98
353	48455	13.73	-100.50
354	48568	7.18	-103.62
355	48694	1.35	-108.18
357	48855	16.05	-103.92
358	48900	10.82	-106.67
375	51777	39.07	-88.05
377	51895	37.85	-91.65
373	51656	41.50	-86.15
388	52681	38.73	-103.10
399	53614	38.42	-106.27
392	52889	36.05	-103.95
382	52391	41.70	-104.03
387	52652	38.43	-100.58
413	54511	39.93	-116.33
414	54534	39.67	-118.12
406	54218	42.27	-118.90
396	53463	40.82	-111.68
421	55591	29.72	-91.04
428	56294	30.68	-104.07
429	56492	28.82	-104.07
447	57518	29.48	-106.33
446	57515	29.50	-106.55
434	56778	25.04	-102.73
445	57494	30.42	-114.28
462	58606	28.67	-115.97
444	57467	30.70	-111.07
448	57679	28.25	-112.85
469	58965	25.07	-121.33
482	59981	16.85	-112.33
484	60119	34.30	-6.60
485	60390	36.72	-3.23
490	61052	13.48	-2.17
492	61642	14.73	17.43

1	2	3	4
493	62011	32.90	-13.28
088	16596	35.83	-14.28
495	62062	32.08	-23.92
496	63206	31.33	-27.22
499	62414	24.03	-32.88
500	62721	15.60	-32.55
502	64650	4.38	-15.03
503	64700	12.13	-18.57
505	65201	6.58	-3.33
506	65578	5.25	3.95
507	70026	71.30	156.78
513	70261	64.82	147.87
514	70273	61.17	149.98
512	70231	62.96	155.62
516	70316	55.90	-162.72
522	70414	52.72	-174.10
523	70409	51.90	176.65
521	70454	52.83	-173.18
524	72201	24.55	81.80
536	72250	25.92	97.47
539	72259	32.83	97.83
535	72248	32.47	93.82
554	72353	35.40	102.20
541	72265	32.93	97.60
538	72253	29.53	98.47
550	72311	33.95	83.32
527	72208	32.90	80.04
551	72317	36.08	79.95
531	72232	32.30	86.40
570	72493	39.10	108.53
569	72469	39.77	104.90
580	72572	40.77	111.97
572	72493	37.73	122.20
560	72392	34.55	120.60
561	72394	34.90	120.45
574	72518	42.75	73.80
634	74496	40.65	73.78
585	72606	43.65	70.32
576	72528	42.93	78.73
593	72722	46.37	75.98

1	2	3	4
578	72553	41.38	93.03
568	72456	39.07	95.62
566	72445	38.97	92.37
588	72655	45.58	94.18
579	72562	41.13	100.70
598	72775	47.50	111.52
597	72775	48.18	106.63
599	72785	47.62	117.52
602	72807	47.30	54.00
604	72815	48.53	58.55
605	72816	53.32	60.42
607	72837	51.27	80.65
609	72867	53.97	101.10
616	72915	64.20	83.37
620	72934	60.03	111.97
626	74043	65.28	126.80
628	74082	76.23	119.33
631	74072	82.50	62.33
617	72917	80.00	85.93
633	74109	50.68	127.37
601	72798	48.38	124.73
611	72896	53.88	122.68
637	76644	20.97	89.52
638	76679	19.40	99.20
640	78016	32.38	64.67
643	78089	24.07	74.53
649	78467	17.93	76.78
650	78467	19.05	69.38
652	78501	17.40	83.93
654	78806	8.97	79.56
655	78867	17.11	61.78
659	78967	10.68	61.35
660	78988	12.22	68.98
661	80001	12.80	81.67
662	80224	4.60	74.08
663	91066	28.22	177.32
664	91115	24.78	-141.33
665	91131	24.28	-153.97
666	91165	21.87	159.35
667	91217	14.96	-144.84
669	91245	19.28	-166.65
670	91250	12.33	-162.33
671	91275	17.33	-169.52
672	91285	19.73	155.07
673	91334	7.45	-151.83

1	2	3	4
674	91348	6.97	-158.22
675	91366	8.72	-167.73
676	91376	7.10	-171.40
679	91700	-2.27	171.72
680	98327	15.17	-120.57
682	99041	45.00	16.00
683	99052	52.50	20.00
684	99061	59.00	20.00
685	99063	62.00	33.00
686	99176	83.10	151.00
688	99185	86.00	49.00
690	99276	79.30	-160.90
693	99360	66.00	-2.00
006	01241	63.70	-9.62
695		32.66	114.60
546	72290	32.73	117.17
544	72274	32.13	110.93
557	72374	35.02	110.73
696	02B	56.50	51.00
697	03C	52.80	35.50
698	04D	44.00	41.00
699	05E	25.00	48.00
700	17P	50.00	145.00
701	24N	30.00	140.00
702	25V	34.00	-164.00
704	41350	-.68	-73.17
706	41350	24.90	-67.13
707	41917	23.77	-90.38
708	42339	26.30	-73.03
709	42339	28.58	-77.20
710	42475	25.45	-81.74
711	42809	22.82	-88.45
712	42867	21.10	-79.05
713	43003	19.12	-72.85
714	43149	17.72	-83.23
715	43279	13.00	-80.18
716	43333	12.67	-92.72
717	43371	8.48	-76.95
729	61401	12.62	8.03
730	61401	25.23	11.62
731	61900	-9.72	14.42
733	61995	-20.30	57.50
734	63450	9.00	-38.73
735	63741	-1.30	-36.75
736	63741	-6.87	-39.20
737	64005	.05	-18.27
738	64210	-4.32	-15.32

1	2	3	4
740	64400	-4.83	-11.90
741	64501	-.70	-8.75
743	64750	9.15	-18.38
745	64870	7.28	-9.72
746	64910	4.02	-13.23
749	66160	-8.85	-13.32
752	67009	-12.28	-49.30
753	67085	-18.90	-47.53
754	67197	-25.03	-46.97
755	67241	-15.02	-28.45
758	67663	-14.47	-40.67
759	67774	-17.83	-31.02
762	81405	4.83	52.37
763	82400	-3.83	32.42
764	82898	-8.02	34.85
765	83781	-23.55	46.63
766	84129	-2.14	79.87
767	84631	-12.10	77.87
769	91334	7.45	-151.83
770	91348	6.97	-158.22
771	91376	7.10	-171.40
772	91408	7.35	-134.48
773	91489	2.00	157.40
774	91517	-9.42	-159.97
775	91643	-8.52	-179.20
776	91680	-17.75	-177.45
777	91843	-21.20	159.77
778	91938	-17.53	149.58
779	94027	-6.72	-147.00
780	94120	-12.43	-130.87
781	94294	-19.25	-146.77
782	94299	-16.30	-118.62
783	94312	-20.38	-149.77
784	94335	-20.67	-140.50
787	96996	-12.08	-96.88
791	60571	31.63	2.25
792	60625	26.97	-1.08
793	60680	22.76	-5.51

REFERENCES

Frazier, H. M., E. R. Sweeton, and J. G. Welsh, 1968: Data processing support to a program for observational and theoretical studies of planetary atmospheres. Progress Report, Travelers Research Center, Inc , Hartford, Conn., 87 pp.

Gilman, P. A., 1965: The mean meridional circulation of the southern hemisphere inferred from momentum and mass balance. Tellus, 17, 277-284.

Holopainen, E. O., 1967: Mean meridional circulation and flux of angular momentum over the northern hemisphere. Tellus, 19, 1-13.

Jeffreys, H., 1926: On the dynamics of geostrophic winds. Q. J. R. M. S., 52, 85-104.

Lorenz, E. N., 1967: The Nature and Theory of the General Circulation of the Atmosphere. World Meteorological Organization, Geneva, 161 pp.

Macdonald, N. J., 1968: Estimates of the seasonal variation of the general circulation from easily identifiable features. Tellus, 20, 300-304.

____, 1969: Estimating the motion and mechanics of a planetary atmosphere. Planetary & Space Sci., 17, 1149-1160.

Macdonald, N. J. and H. M. Frazier, 1969: A note on the seasonal variation of the flux of angular momentum by the transient and standing eddies in the northern hemisphere. Tellus, 21, 656-667.

Mintz, Y., 1951: The geostrophic poleward flux of angular momentum in

the month of January 1949. Tellus, 3, 33-46.

Palmen, E. and L. A. Vuorela, 1963: On the meridional circulations in the northern hemisphere during the winter season. Q. J. R. M. S., 89, 131-138.

Priestly, C. B., 1949: Heat transport and zonal stress between latitudes. Q. J. R. M. S., 75, 28-40.

Priestly, C. B. A. J. Troup, 1964: Strong winds in the global transport of momentum. J. Atmos. Sci., 21, 459-460.

Rosen, R. D., 1970: Generation and vertical transport of zonal kinetic energy. S. M. Thesis, Dept. of Meteorology, M. I. T., 126 pp.

____, 1971: Vertical transport of mean zonal kinetic energy for five years of hemispheric data. Submitted to Tellus.

Shenk, W. E. and E. R. Kreins, 1970: A comparison between observed winds and cloud motions derived from satellite infrared measurements. J. Appl. Meteor., 9, 702-710.

Sims, J. E., 1969: Evaluation of the symmetrical zonal kinetic energy equation. S. M. Thesis, Dept. of Meteorology, M. I. T., 84 pp.

____, 1970: Meridional transport of mean zonal kinetic energy from 5 years of hemispheric data. Tellus, in press.

Starr, V. P., 1951 : A note on the eddy transports of angular momentum. Q. J. R. M. S., 77, 44-50.

____, 1968: Physics of Negative Viscosity Phenomena. McGraw Hill Book Co., New York, 254 pp.

Starr, V. P. and N. E. Gaut, 1969: Symmetrical formulation of the zonal kinetic energy balance equation. Tellus, 21, 185-192.

____, 1970: Negative viscosity. Scientific American, 223, 72-80.

Starr, V. P., J. P. Peixoto, and N. E. Gaut, 1970: Momentum and zonal kinetic energy balance of the atmosphere from five years of hemispheric data. Tellus, 22, 251-274.

Starr, V. P., J. P. Peixoto, and J. E. Sims, 1970: Method for the study of the zonal kinetic energy balance in the atmosphere. Pure and Appl. Geoph., 80, 346-358.

Starr, V. P. and B. Saltzman, 1966: Observational Studies of the Atmospheric General Circulation. Sci. Rep. No. 2, M. I. T. Planetary Circulations Project, Contract No. AF19(628)-5816, 700 pp.

Starr, V. P. and J. E. Sims, 1970: Transport of mean zonal kinetic energy in the atmosphere. Tellus, 22, 167-171.

Starr, V. P. and R. M. White, 1951: A hemispherical study of the atmospheric angular momentum balance. Q. J. R. M. S., 77, 215-225.

____, 1952: Schemes for the study of hemispheric exchange processes. Q. J. R. M. S., 78, 62-69.

Tucker, G. B., 1959: Mean meridional circulations in the atmosphere. Q. J. R. M. S., 85, 209-224.

Vuorela, L. A. and L. I. Tuominen, 1964: On the mean zonal and meridional circulations and the flux of moisture in the northern hemisphere during the summer season. Pure and Appl. Geoph., 57, 167-180.

Walker, H. C., 1969: The effect of an unbiased grid in determining the kinetic energy balance of the northern hemisphere. S. M. Thesis, Dept. of Meteorology, M. I. T., 81 pp.

____, 1970: Unbiased station grid for study of the kinetic energy balance of the atmosphere. Pure and Appl. Geoph., 81, 313-322.

White, R. M., 1949: The role of mountains in the angular momentum balance of the atmosphere. J. Meteor. 6, 353-355.

Widger, W. K., 1949: A study of the flow of angular momentum in the atmosphere. J. Meteor., 6, 291-299.

ACKNOWLEDGEMENTS

The author wishes to express his gratitude to Professor Victor P. Starr for suggesting the topic and the Professor Edward N. Lorenz for reading the manuscript and making some helpful suggestions on the related material. Special thanks are due to Mr. Laurence Reed of Travelers Research Center, Inc. for performing the calculations. The writer also wishes to thank his fellow students Richard Rosen and Air Force Majors David Ferruzza and Hans Fischer for their useful advice and comments.

This research was supported by the National Science Foundation under Grant No. GA-1310X. My attendance at M.I.T. was sponsored by the U.S. Air Force through the Air Force Institute of Technology.

Appreciation is extended to Mrs. Barbara Goodwin for typing the manuscript and to Miss Isabelle Kole for drafting the figures.